ANALYSIS OF WELL TEST DATA IN THE OLKARIA WEST GEOTHERMAL FIELD, KENYA

Charles B. Haukwa*
UNU Geothermal Training Programme
National Energy Authority
Grensasvegur 9, 108 Reykjavik
ICELAND

*Permanent address:
The Kenya Power Company Ltd.
Olkaria Geothermal Project
P.O. Box 785, Naivasha
KENYA

ABSTRACT

Analysis of transient pressure tests for Olkaria West wells shows that both infinite acting and double porosity models can be used to analyse the well behaviour and infer reservoir properties from fall-off steps of long enough duration, in wells where no significant thermal recovery occurs. The double porosity model gives better estimates of reservoir properties than the infinite acting model, for long fall-off steps in wells intercepting fractures. Semilog methods give fairly good estimates of reservoir transmissivity for the long fall-off steps but are highly inaccurate when used independently, especially for the short fall-off steps conducted in most of the wells.

Double porosity models can also be used for recovery test analyses where two phase transients are not siginificant, but semilog methods are more practicable for the long recovery steps conducted as long as the end of the two phase condition can be identified by considering the effect of Carbon dioxide.

The depletion study of the entire Olkaria reservoir area shows that only 22% of the fluid mass remains after 35 years of production with an average output equivalent to 250 MWe, using an effective porosity of 2%. Dry steam is produced from most of the areas after 20 years.

TABLE OF CONTENTS

LIST OF TABLES

LIST OF FIGURES

NOMENCLATURE

b	:	average width of fracture
C	:	wellbore storage coefficient m^3/Pa
c	:	compressibility 1/Pa
F	:	defined by Eq (21)
h	:	reservoir thickness m
k	:	permeability m^2
K	:	Modified Bessel function of the second kind
m	:	defined by Eq (29)
m	:	slope of semilog line Pa/cycle
n	:	number of fractures
n	:	mass concentration kg/kg
P	:	pressure Pa
ΔP	:	pressure change Pa
$\bar{P}$	:	Laplace transform of P
q	:	flow rate m^3/s
Q	:	flow rate l/s
r	:	radial distance m
s	:	skin factor
s	:	Laplace transform
S	:	formation storage m/Pa
t	:	time s
Δt	:	time change s
T	:	temperature °C
T	:	transmissivity m^3/Pas
x	:	fracture half length m
V	:	volume m^3

Greek symbols

λ	:	defined by Eq (27)
μ	:	dynamic viscosity Pas
ϕ	:	porosity
ω	:	defined by Eq (27)
γ	:	defined by Eq (29)
τ	:	defined by Eq (29)
ρ	:	density kg/m^3

Subscripts

D,d	:	dimensionless
e	:	effective
f	:	fracture system
m	:	matrix system
s	:	skin zone
t	:	total
w	:	wellbore
x	:	based on fracture half length

1 INTRODUCTION

1.1 Scope of work

The author was granted a UNU Fellowship to study reservoir engineering at the 1985 UNU Geothermal Training Programme held at the National Energy Authority in Reykjavik Iceland.

The training programme began with introductory lectures for six weeks on all aspects of geothermal energy development and utilization which included geology, geophysics, geochemistry, drilling, reservoir engineering and electrical and non-electrical uses. This was followed by eight weeks of specialized training in reservoir engineering and borehole geophysics. Before commencing the work presented in this report, two weeks of field excurssion and seminars on various Icelandic geothermal fields was undertaken.

The report covers analysis of well test data from the Olkaria West exploration area, with specific emphasis on transient pressure tests. The data used on this aspect of the report was collected by the author in his work as Measurements Engineer for the Olkaria Geothermal Project. A depletion study of the entire Olkaria field was subsequently undertaken using reservoir permeability values from the transient pressure analyses.

The topics chosen and the emphasis put on particular aspects were purposely aimed to provide the author with useful practical knowledge on application of different well test analysis methods and methods used in computer simulation of geothermal reservoirs. The computer programmes used in the transient pressure analyses were written by Ragnar Sigurdsson and Omar Sigurdsson, both at the National Energy Authority.

2 THE OLKARIA GEOTHERMAL FIELD

2.1 Geological structure

The Olkaria geothermal field is located within the East African rift system, to the south of lake Naivasha, at an altitude of about 2000 m. The aerial extent of the field as defined by a resistivity anomally is approximately 100 km^2. Initial field development was concentrated in an area of 4 km^2 located to the south-east and referred to as Olkaria East. The development proceeded in small stages with the commissioning of the first 15 MWe turbine in 1981. To date 25 wells have been drilled in this area and three 15 MWe turbines are currently installed with available steam sufficient for 50 MWe.

The Olkaria East field is underlain by a 250-300°C boiling reservoir at depths below 800 m which is capped by a 240°C steam cap of varying thickness from 50 to 250 m. The pressure within Olkaria East increases northwards and the steam cap diminishes as indicated by well 26 (KPC 1984a).

Trachyte lavas and tuffs with generally low permeability, constitute the boiling reservoir , with most of the steam produced from fractures and joints in the basaltic and pyroclastic horizons at 500-800 m depth.

Production capacity of the Olkaria East wells is low, on average 1-3 MWe with the highest production corresponding to 6 MWe from well 16. Transient pressure tests on these wells indicate average transmissivity of 1.0-2.0E-08 m^3/Pas (Table 1), but recent history match of production (KPC, 1984b), indicates higher permeability. Production causes boiling within the reservoir and the average enthalpy of productive wells is 2000-2600 KJ/kg.

In order to delineate the Olkaria geothermal field and define a new area for development seven wells have been drilled to the north and north-west of the present field (Fig. 1), referred to as Olkaria West. However, at the time of writing this report data from only six of these wells is available, and is summarized below.

2.2 Summary of well test data

Well 101: This was the first well to be drilled in Olkaria West under the exploration programme and was sited to the west of the Olkaria fracture zone. The well was completed on 7/3/82 to a depth of 1616 m. The production casing is set at 632 m and loss zones below casing shoe were encountered at 640, 910-990 m, with total loss of circulation at 1020 m. Below 1040 m, aerated foam was used with loss zones detected at 1320-1350 and 1520-1530 m. This was further confirmed by completion tests, pressure and temperature recovery, and flowing temperature/pressure profiles which indicate the major permeable zones to be at 632-700, 800, 900-1050, 1150 and below 1500 m. The well cuts through a near vertical fracture zone in the interval 640 to 1500 m.

The four step injection test was conducted at 1000 m after thewell had been under continuous cold water injection for over eight hours, with the last step of 27.3 l/s lasting fifty two minutes. Injectivity increases with injection rate and exceeds 5.0 l/s/bar, butinjection steps lasted only 45-55 minutes and this value of injectivity could have been influenced by wellbore storage. The fall-off step lasted 41 minutes, but the well recovers very rapidly in temperature at 650-750 m and non-isothermal effects probably influence the result of the fall-off step.

Prior to major well discharge, the maximum temperature was 232°C at 800 m with an average of 203°C at 900-1400 m and a bottom hole temperature of 232°C.

Results of discharge, show the average output to be 10.3-13.3 kg/s with enthalpy of 1260-1640 KJ/kg at 6.5 bara WHP. However, these results were certainly influenced by the large water carry over from the concrete wall silencer. The discharge lasted 387 days and a flowing pressure profile prior to shut in showed a drawdown of 30 bars at 1000 m. When the well was shut in it recovered to 99% of the maximum recorded pressure at 1000 m in about four and a half hours. Pressure was monitored for a further 55 days but showed excessive fluctuation probably because of WHP leakage. The maximum pressure at 1000 m after one year of

shut in following discharge is 52.3 bara and temperature runs show that temperatures have recovered considerably. The maximum temperature is 252°C at 1580 m while the temperature at 1000 m is 236°C.

Current output tests on this well using a cyclone silencer show an average discharge enthalpy of 1085 KJ/kg, with a mass output of 15.1 kg/s at a WHP of 6.6 bara using a 4" lip pipe. The average output after a further 45 days of discharge on 5" lip pipe was 16.3 kg/s at 5.3 bara and 1085 KJ/kg enthalpy. Thus it is not clear how much of the observed higher enthalpy during the first test was due to water carry-over or actual boiling in the reservoir caused by the observed drawdown during discharge. This has to be confirmed by the current discharge test over a similar period. However, by comparison with other Olkaria West wells the value of the current discharge enthalpy has been used to correct previous test results and recalculate transmissivity.

Well 201: This well was completed to 2116 m on 25/3/83 and had been heating for 2 days prior to completion tests. Indicated aquifers from completion tests, losses during drilling,and chemical analysis of circulation fluids, are at 960-1000, 1080-1120, 1220-1260 m, with minor aquifers at 1340-1350, 1456-1460, 1600-1700 m, and at 1900 m. This well, is located on the Olkaria fault and cuts through fractures in the interval 960 to 1460 m. Injectivity increases with injection rate and exceeds 1.67 l/s/bar, but injection steps lasted one hour on average except the first step which lasted 5.5 hours. Following 20 hours of cold water injection, injection was stopped for 24 hours followed by a single step injection of 25.2 l/s for 160 minutes and a fall-off step of 60 minutes, with the pressure instrument located at 1900 m.

Temperature recovery shows a maximum of 237°C at 1000 m with an average of 225°C at 1200-1800 m and a bottomhole temperature of 193°C. The well mass output is 34.2 kg/s at 4.5 bara WHP with average enthalpy of 1085 KJ/kg, but slight water carry over probably influences the results.

Following 281 days of discharge at various rates with the last rate lasting 84 days, the well was shut in and pressure recovery monitored continuously at 1000 m for 4 hours, followed by further recovery monitoring for 35 days. The pressure at 1000 m recovered to 97% of the maximum measured value in only 40 minutes and reached the maximum value in 6 days, followed by a reduction which fluctuated. After 86 days of shut in the pressure at 1000m was 39.2 bara with temperature of 235°C. A repeat discharge test on this well shows no change from previously measured values.

Well 301: Well 301 was completed to a depth of 1912 m on 3/10/83. During drilling from anchor casing at 333 m, circulation loss was encountered at 350 m and drilling continued with no returns. At a depth of 520 m, steam discharge started and continued to 658 m, when a return fluid discharge with WHP of 4.2 bara was maintained, while pumping in 16.7 l/s of cold water. A discharge test at this depth showed that the well produced in excess of 25 kg/s with estimated enthalpy of 1600 KJ/kg at a WHP of 6.3 bara, but gas sampling showed 50% of the steam discharge was CO_2.

A pumping test at this depth showed the well had very large permeability (no measurable increase in pressure with increase in pump rate). The casing shoe was set at 519 m and the well drilled to 1912 m, with continuous steam discharge.

The well had been heating for nearly 24 hours when completion tests began. Indicated aquifers are at 520-650, 900-1000 and 1250-1350 m. The pressure pivot point indicates that the major aquifer is at 1200-1300 m. Injectivity increases with injection rate and exceeds 4.33 l/s/bar, but injection steps were not continuous due to problems with water supply. The last injection step lasted 70 minutes at a pump rate of 31.6 l/s followed by a fall-off step for 42 minutes, conducted at 1000 m after a total injection period of 9.5 hours with some interruptions. The well was located on the Olkaria fault and cuts through a near vertical fracture zone in the interval 520 to 1500 m.

Temperature recovery shows a maximum of 300°C at 1895 m and an average of 225-235°C over the interval 520-1300 m where the highest permeability is encountered.

Long term discharge testing of this well has not been possible mainly due to environmental constraints on waste water disposal. The short discharge test conducted in March 1985 showed that the well produced in excess of 65 kg/s with enthalpy of 1575 KJ/kg at WHP of 22.5 bara, using two silencers with 6", and 8" discharge pipes in parallel. However, the output dropped rapidly to 34 kg/s with enthalpy of 1725 KJ/kg at WHP of 6.3 bara, when two 8" discharge pipes were installed. On both tests accurate determination of discharge enthalpy was not possible due to enormous quantities of carry over water from the silencers. However, the tests show that using larger discharge lines probably causes flashing within the formation around the wellwhich impedes liquid flow. The measured CO_2 content of this well is much higher than encountered in any other well in Olkaria and the rapid reduction in output could also be due to calcite deposition either in the well or the formation. A long term discharge test is currently under way but no results are available.

Well 401: This well was completed to a depth of 2505 m on 21/4/84 and had been heating for about 13 days prior to completion tests. Aquifers were identified at 1000-1200 and 1800-1900 m. Pressure pivot point indicates the main active aquifer to be at 1200 m, while temperature recovery indicates an aquifer cased off at 800 m (casing shoe at 877 m).

The first fall-off step was conducted at 1100 m after continuous cold water injection at various rates for over 20 hours with the last rate of 26.9 l/s lasting 2.5 hours. The fall-off step lasted 2 hours. The second fall-off step was conducted one week later at 1000 m, after a three step injection test using 12.3, 17.4, and 27.9 l/s for two hours each. The fall-off step lasted 130 minutes.

Temperature recovery shows a maximum of 225°C at 800 m, and a bottom hole temperature of 208°C with an average of 200-208°C over the 900-2000 m interval.

Discharge test shows the well has a mass output of 22.8 kg/s at 4.9 bara WHP with enthalpy of 985 KJ/kg, but the large water carry over certainly influences this result. Assuming the well discharges at saturated enthalpy corresponding to 205°C (875 KJ/kg), the output is 25.9 kg/s, this discharge rate being equivalent to a water carry over of 20%. No shut in test has been conducted on this well.

Well 501: This well was completed to a depth of 1801 m on 16/12/84, and had been heating for over 22 hours prior to completion tests. The major aquifer as inferred from losses of circulation and temperature profiles during pumping is at 1390-1500 m, with a minor aquifer at 1140 m. The well cuts through a near horizontal fracture at 1390 m. Injectivity increases with injection rate and exceeds 3.33 l/s/bar.

The first fall-off step was conducted at 1400 m after continuous cold water injection for 13.5 hours with 13.3 l/s for 4 hours followed by 22.5 l/s for 9.5 hours. The fall-off step lasted 5 hours and was followed 1.5 hours later by a four step injection test lasting a total of 11.5 hours. This was followed by a second fall-off step which lasted 8 hours.

Temperature recovers very rapidly below 1390 m and exceedes 285°C at well bottom, but the average over the interval 500-1300 m is 130°C. The well has not been successfully brought to discharge because of the cold water column above 1390 m.

Well 601: This well was completed in early January 1985, to 2600 m depth, but no major aquifers were intercepted. The well was drilled away from known faults in the area and the maximum temperature after heating for 3 months is 325°C at 2590 m.

2.3 Pressure and temperature distribution

Fig. 1 also shows the isobars and isotherms at 1000 masl within the Olkaria geothermal field. Most of the wells in both East and West Olkaria except wells 501 and 601 have permeable zones within this interval. The pressure and temperature in East Olkaria increases northwards, while that in West Olkaria increases westwards. Both wells 201 and 401 which penetrate to depths in excess of 2 km do not encounter high temperatures at depth, but show near saturated temperatures at depths of 1000 m and 800 m respectively, caused by lateral flow. Olkaria well 101 shows saturated conditions around 640 to 800 m, with considerable departure from saturated conditions below. Olkaria well 1 drilled 2.5 km SE of well 401 and 4 km SW of the present production field, encounters only 126°C at 1000 m. Well 501 encounters high temperatures below 1390 m where an aquifer was intercepted. Well 601 encounters more than 325°C at 2.5 km, but no aquifer was intercepted. Thus, in Olkaria West, the drilled wells indicate that most permeability is in the single phase liquid reservoir which is further confirmed by the low discharge enthalpy of these wells.

2.4 Hydrological model

The temperature and pressure distribution observed above suggests a hydrological division between the eastern and western part of greater Olkaria. The Olol-Butot fault forms the eastern boundary, while the Olkaria fracture zone forms the western boundary of this dividing zone. This dividing zone drains from the eastern and western Olkaria and from shallow outflow of Lake Naivasha which apparently forms the cold component. Both well 201 and 401 are connected laterally to the western system. If this is so then the western system obtains its recharge from deep drainage along the western scarp, while the eastern system obtains its recharge mainly by deep drainage from Lake Naivasha.

2.5 Review of past simulations

To date four simulations of the performance of the East Olkaria geothermal field have been carried out. The first was in 1980 by Bodvarsson (KPC,1980) using a vertical model and dealt mainly with the effects of vertical permeability and the effects of exploitation levels on field life. The main conclusion was that production from the steam zone alone limited productive life.

The second simulation by Bodvarsson (KPC 1981), showed that productive capacity is greatly affected by horizontal and vertical permeability. If the values of horinzotal permeability were as small as measured by transient tests then 45 Mwe could not be supported without extension of the production area.

A study by Waruingi (1982), using a two dimensional aerial model showed the area could only support 30 Mwe for 12 years using the measured values of permeability.

A detailed study by Bodvarsson (KPC 1984a), involved a history match with the production data to obtain effective values for reservoir permeability and porosity which were then used to predict future performance. In general the results show higher permeabilities than inferred from well tests, indicating an average permeability of 7.5 md for the steam zone and an average of 4 md for the liquid zone. Inferred values of transmissivity from this simulation are shown in Table (1), along with the measured ones.

Performance prediction shows that for 45 Mwe for 30 years, the area has to be extended by 2.3 km^2. Generation of 105 Mwe requires an area of 9.5 km^2, with injection greatly reducing the required area.

3 WELL TESTING

3.1 Types of well tests

Various tests are usually carried out on geothermal wells to determine individual well and overall field perfomance. The parameters obtained during individual well tests and interference tests between wells are primary inputs into the reservoir model which can be used to predict field performance.

In the upper parts of the well, before production casing is run, one is mainly interested in formation static temperature and pressure profiles. Static pressures can be measured whenever loss circulation occurs. However, measurement of actual static formation temperatures may involve halting of drilling operations for several days. Therefore several methods are used to estimate the temperature. This can be combined with study of cores and cuttings for high temperature alteration minerals and is necessary for isolation of low temperature shallow feeds prior to setting production casing.

The tests that are carried out at the completion of a well depend on the information required and the available instrumentation. In Iceland for example, these tests include transient pressure tests, injectivity, formation logs (NN porosity, γ-γ density, nat-γ lithology), resistivity, caliper logs, differential temperature, temperature and pressure profiles. In Olkaria the tests include transient pressure, injectivity, water loss (using spinner and temperature instruments) and temperature and pressure profiles.

After completion tests, the well is allowed to recover in temperature and pressure with regular monitoring. This is followed by a discharge test which lasts up to several months, to establish well output characteristics.

The discharge test is followed by a shut-in test in which pressure recovery is monitored for up to two months, in the shut-in well. To date no interference tests have been carried out in Olkaria.

In this report, transient pressure tests of five exploration wells in the Olkaria West field are analysed using all standard transient pressure analysis methods to obtain values of reservoir transmissivity and near well formation properties. The tests include fall off steps following cold water injection and recovery following discharge.

3.2 Objectives of transient pressure tests

The objectives of transient pressure tests in geothermal wells are:

1. Measurement of average transmissivity, mean formation pressure and formation storage. These are primary inputs into reservoir simulators, and can also be used to estimate well productivity.

2. Determination of skin effect, which can be used to decide if the well can be improved by stimulation.

3. Determine the well flow characteristics and near well reservoir characteristics e.g the influence of fractures, leaky or impermeable boundaries and where possible shape or size of the drainage area.

4. Determine optimum well test design e.g duration of test steps to get beyond the wellbore storage period and minimize nonisothermal effects.

3.3 Typical completion test programme for Olkaria wells

Various combinations of completion test programmes have been used at Olkaria and injection steps used on some of the earlier wells have been as short as 20-40 minutes. At present a standard test programme at completion is as follows.

1) Water loss test using temperature instrument at low pump rate; 2) Spinner flowmeter run at low pump rate; 3) Spinner profile while pumping at high pump rate; 4) Temperature profile while pumping at high pump rate; 5) Step injection test followed by a fall off test.

In the water loss test, the movement of cold injected water is monitored with a series of temperature profiles during pumping. This test lasts about five hours and requires that the well be allowed to recover in temperature for about one to three days following completion of drilling before it is conducted, in order to identify the upper loss zones in the well. The spinner flowmeter runs during water injection have been used with little success due to erratic records and the fact that no caliper logs of the open hole were taken to aid in the interpretation of the spinner speed records. For some of the wells, the step injection tests have been split. Some of the injection steps have been taken simultaneously with or between tests 1-4 above, with the last step injection test consisting of only two steps at higher pump rates followed by the fall-off step. The injection steps last on average 2-3 hours while the fall-off step lasts 2-5 hours.

4 THEORY OF TRANSIENT PRESSURE TESTING

4.1 Theis solution

The basic equation describing flow of a single phase fluid through porous media is a combination of Darcy's law, conservation of mass and an equation of state. It is called the diffusivity equation and can be written in radial coordinates as:

$$\frac{\partial^2 P}{\partial r^2} + \frac{1}{r} \cdot \frac{\partial P}{\partial r} = \frac{\phi \mu c_t}{k} \frac{\partial P}{\partial t} \qquad (1)$$

Assumptions inherent in this equation are horizontal flow (fully penetrating well), negligible gravity effects, the medium is homogenous and isotropic, with constant permeability, porosity and thickness; pressure gradients are small and fluid flow is isothermal with constant viscosity and compressibility. In dimensionless terms equation 1 becomes:

$$\frac{\partial^2 P_D}{\partial r_D^2} + \frac{1}{r_D} \cdot \frac{\partial P_D}{\partial r_D} = \frac{\partial P_D}{\partial t_D} \qquad (2)$$

where: $P_D = \frac{2\pi kh\Delta P}{q\mu}$; $t_D = \frac{kt}{\phi \mu c_t r_w^2}$; $r_D = \frac{r}{r_w}$

This is the basic equation for well testing and can be solved for various boundary conditions and modified to account for assumptions above which become invalid, (Kjaran and Elliasson 1983; Earlougher 1977; Lee 1982).

One solution is the continous line source solution for an infinite reservoir where the well is represented as a line source so the initial and boundary conditions are:

$$P_D = 0 \quad \text{at} \quad t_D = 0 \quad \text{for all} \quad r_D$$
$$P_D = 0 \quad \text{at} \quad r_D = \infty \quad \text{for all} \quad t_D > 0$$

$$\lim_{r_D \to o} \left(\frac{\partial P_D}{\partial r_D}\right) = -1 \qquad t > 0$$

The solution to the diffusivity equation with these inititial and boundary conditions is the exponential intergral solution, also known as the Theis solution:

$$P_D(r_D,t_D) = - 0.5E_i(-r_D^2/4t_D) \qquad (3)$$

The logarithmic approximation to Eq 3 in SI units is given by:

$$\Delta P = 0.1832\frac{q\mu}{kh}\left[\log\frac{kt}{\phi\mu c_t r^2} + 0.3514\right] \qquad (4)$$

and is accurate to 2% if $t_D/r_D^2 > 100$ or $t_D/r_D^2 > 0.5$ for $r_D > 20$.

Equation 4 is widely used in well test analysis where wellbore storage and skin are unimportant as in observation wells, during interference testing.

For a well of finite radius the assumption of a line source well is not always valid and the wellbore boundary condition becomes:

$$\left(r_D\frac{\partial P_D}{\partial r_D}\right) = -1 \qquad t_D > 0$$

$$P_D = 0 \quad \text{at } t_D = 0 \text{ for } r_D > 1$$

with the outer boundary condition remaining unchanged. The solution is:

$$P_D(t_D,r_D) = \frac{2}{\pi}\int_0^\infty (1-e^{u^2t_D})\frac{[J_1(u)Y_o(ur_D)-Y_1(u)J_o(ur_D)]}{u^2[J_1^2(u) + Y_1^2(u)]}du \qquad (5)$$

where $u = \frac{r_D^2}{4t_D}$ and J_o, J_1, are Bessel functions of first kind and order 0,1

Y_o, Y_1, are Bessel functions of second kind and order 0,1

When $r_D > 20$ and $t_D/r_D^2 > 0.5$ or $t_D > 25$ for $r_D = 1$, the above solution reduces to the exponential intergral, with the same logarithmic approximation of equation 4.

4.2 Wellbore storage and skin effects

a) Wellbore storage

During injection of water into a well, fluid inflow into the well does not equal outflow to the formation at all times. Similarly during discharge of a well the inflow from the formation does not equal outflow from the well at all times. For example, when a well is shut-in fluid continues to flow from the reservoir into the well. These effects are called wellbore storage, measured by the wellbore storage coefficient, which is proportinal to the effective wellbore radius (i.e wellbore volume) and fluid compressibility. Presence of vugs and fissures greatly increases wellbore storage capacity.

Thus it is necessary to correct data for wellbore storage where the solution does not take into account wellbore storage, by calculating the sand face flow:

$$q_{sf} = q\left(1 - C\frac{dP_w}{dt}\right) \qquad (6)$$

For a well with a free water level, the wellbore storage coefficient C can be approximated by:

$$C = Vu/\rho g \quad \text{where } Vu = \pi r^2 h;\ h = 1 \text{ meter} \qquad (7)$$

A log-log plot of ΔP vs Δt has a linear unity slope characterising the wellbore storage period from which the actual value of C can be calculated.

The dimensionless wellbore storage coefficient C_D is defined as the ratio between wellbore storage and formation storage:

$$C_D = \frac{C}{2\pi\phi c_t h r^2} \qquad (8)$$

Thus to account for wellbore storage in a well of finite radius, the wellbore boundary condition for the radial diffusivity equation is:

$$\left(r_D \frac{\partial P_D}{\partial r_D}\right)_{r_D \to 1} = -1 - C_D \frac{\partial P_D}{\partial t_D} \qquad (9)$$

b) Skin effects

Quite often there is a zone near the wellbore in which the permeability is altered due to drilling, precipitation of solids during flashing in the formation or presence of fractures. This zone is called the skin zone and to account for it the effective wellbore radius is defined such that:

$$r_e = r_w e^{-s} \qquad s = \text{skin factor} \qquad (10)$$

thus, a positive skin represents a well of effectively narrow radius with increased pressure drop from reservoir to the wellbore, whereas a negative skin represents a well of effectively large wellbore radius with decreased restriction to the fluid flow.

c) Analytical solution

The solution for unsteady liquid flow, including wellbore storage and skin, for an infinite acting reservoir is given by Agarwal et al (1970), in Laplace space by:

$$\bar{P}_{wD} = \frac{K_o(\sqrt{s}) + S(\sqrt{s})K_1(\sqrt{s})}{s\left[(\sqrt{s})K_1(\sqrt{s}) + C_D s\left[K_o(\sqrt{s}) + S(\sqrt{s})K_1(\sqrt{s})\right]\right.} \qquad (11)$$

The above equation is solved by numerical inversion of the Laplace transform in the infinite acting reservoir analytical model, used for fitting transient pressure data, using a computer programme.

d) Logarithmic approximation

The complexity inferred in the solutions to the radial diffusivity equation with wellbore storage and skin only refers to small times for large C_D . For large times or small C_D, the logarithmic approximation in SI units is:

$$\Delta P = 0.1832\frac{q\mu}{kh}\left[\log\frac{kt}{\phi\mu c_t r^2} + 0.3514 + 0.8686s\right] \quad (12)$$

This logarithmic approximation is valid with error of less than 2% for $t_D/r_D^2 > 25$.

For drawdown and injection testing, the time to expect the beginning of the semilog straight line described by Eq 12 is:

$$\Delta t > \frac{(9.55 + 0.557s)C}{kh/\mu} \quad \text{or} \quad t_D > (60 + 3.5s)C_D \quad (13)$$

For fall-off and recovery testing this time is given by:

$$\Delta t > \frac{7.96}{\frac{Kh}{\mu}} C e^{0.14s} \quad \text{or} \quad t_D > (50 C_D\, e^{0.14s}) \quad (14)$$

4.3 Semilog analysis

4.3.1 The MDH method

Taking equation 12 as the basic equation for logarithmic approximation of the solution to the radial diffussivity equation, a plot of P vs t on lin-log scale is called the MDH plot and has a slope m given by:

$$m = 0.1832q(\mu/kh) \quad (15)$$

from which the transmissivity $T = kh/\mu = 0.1832q/m$ can be calculated.

The skin factor s can be calculated by rearrangement of equation 12, if porosity and compressibility are known.

$$s = 1.15\left[\frac{\Delta P}{m} - \log\frac{k}{\phi\mu c_t r_w^2} - 0.3514\right] \qquad (16)$$

For observation wells, located at some distance from the active well the skin factor can be assumed to be zero and hence formation storage S can be obtained by rearrangement of Equation 12 thus:

$$S = 2.246Tt_o/r^2 \qquad (17)$$

where t_o is obtained by extrapolating the MDH semilog straight line to zero P.

4.3.2 The Horner method

By using the principle of superposition the condition that occurs when a production or injection well is shut in can be simulated . The well is assumed to produce/inject continuously at flow rate q for a period t + Δt. At time t, a flow -q is added to simulate the shut in condition. The total response is simply the summation of the effect of q for time t + Δt and -q for a time Δt. The exponential intergral solution, Grant et al (1982), becomes:

$$\Delta P = -\frac{q\mu}{2\pi kh}E_i\left(\frac{\phi\mu c_t r^2}{4k(t+\Delta t)}\right) + \frac{q\mu}{2\pi kh}E_i\left(\frac{\phi\mu c_t r^2}{4k\Delta t}\right) \qquad (18)$$

with the logarithmic approximation given by:

$$\Delta P = 0.1832\,\frac{q\mu}{kh}\log\left(\frac{t+\Delta t}{\Delta t}\right) \qquad (19)$$

A lin-log plot of ΔP vs (t + Δt)/Δt has slope m given by equation 15 from which T can be calculated.

4.4 Wells intercepting fractures

For wells intercepting fractures, the radial diffusivity equation still applies, with the wellbore boundary condition replaced by the fracture boundary condition.

The infinite conductivity vertical fracture solution assumes no pressure drop along the fracture plane at any instant in time and is given by Gringarten el al (1974) as:

$$P_{wD}(t_{Dxf}) = \frac{1}{2}\sqrt{\pi t_{Dxf}}\left[ERF\left(\frac{0.134}{\sqrt{t_{Dxf}}}\right) + ERF\left(\frac{0.866}{\sqrt{t_{Dxf}}}\right)\right]$$

$$- 0.067Ei\left(\frac{-0.018}{t_{Dxf}}\right) - 0.433Ei\left(\frac{-0.750}{t_{Dxf}}\right) \qquad (20)$$

where $t_{Dxf} = \dfrac{kt}{\phi\mu c_t x_f^2}$

For large values of time $t_{Dxf} > 3$, the logarithmic approximation is:

$$P_{wD}(t_{Dxf}) = 0.5\ln(t_{Dxf}) + 1.1 \qquad (21)$$

For small values of time $t_{Dxf} < 0.016$, usually called the linear flow period, the approximation is:

$$P_{wD}(t_{Dxf}) = \sqrt{\pi t_{Dxf}} \qquad (22)$$

Thus, a half slope on a log-log plot of ΔP vs Δt, for early times characterizes the presence of a fracture.

The uniform flux fracture solution assumes the fluid enters the fracture at a uniform flow rate per unit area of fracture face and is also given by Gringarten et al (1974) as:

$$P_{wD}(t_{Dxf}) = \sqrt{\pi t_{Dxf}}\ ERF\left(\frac{1}{2\sqrt{t_{Dxf}}}\right) - \frac{1}{2}Ei\left(-\frac{1}{4}t_{D}x_f\right) \qquad (23)$$

For large values of time $t_{Dxf} > 2$ the approximation is:

$$P_{wD}(t_{Dxf}) = 0.5\left(\ln(t_{Dxf}) + 2.8091\right) \qquad (24)$$

and for small values of time $t < 0.16$ the approximation is:

$$P_{wD}(t_{Dxf}) = \sqrt{\pi t_{Dxf}} \qquad (25)$$

The solution for a finite conductivity uniform flux vertical fracture is given by Reynolds et al (1982), in Laplace space as:

$$\bar{P}_{wD} = \frac{\pi}{h_{fD}F_{CD}} \cdot \frac{1}{\left[\frac{h_{fD}C_{fD}s + 2\sqrt{s}}{h_{fD}F_{CD}}\right]\tanh\left[\frac{h_{fD}C_{fD}s + 2\sqrt{s}}{h_{fD}F_{CD}}\right]} \qquad (26)$$

where $F_{CD} = \frac{k_f b_f}{k x_f}$; $h_{fD} = \frac{h_f}{h}$; $C_{fD} = \frac{\phi_f b_f}{\phi x_f}$

This equation is solved by numerical inversion of the Laplace transform in the finite conductivity vertical fracture model used for fitting transient pressure data, after correcting for wellbore storage using equation 6.

4.5 Double porosity systems

Naturally fractured reservoirs are described with double porosity systems, where most of the reservoir fluid is stored in matrix blocks which have generally low permeability, whereas the fractures and openings in the blocks form vugs and interconnected channels of high permeability, but very low storativity, (Da Prat (1982), Moench (1983). Therefore most of the fluid transport takes place in the fissures with the blocks acting as fluid sources. To take this into account Warren and Root (1963), defined the interporosity flow coefficient λ and the relative fracture storativity ω as follows:-

$$\lambda = \alpha r_w^2 \frac{k_m}{k_f}; \qquad \omega = \frac{(\phi c_t)_f}{(\phi c_t)_f + (\phi c_t)_m} \qquad (27)$$

The solution to the radial diffussivity equation for block to fissure flow in an infinite double porosity system, with wellbore storage, skin and fracture skin, is given by Moench (1983), for a fully penetrating well tapping a horizontal fracture, confined above and below by impermeable barriers. In Laplace space the solution becomes:

$$\bar{P}_{wD} = \frac{K_o(\sqrt{s+\bar{q}_D}) + S(\sqrt{s})K_1(\sqrt{s+\bar{q}_D})}{s\left[(\sqrt{s+\bar{q}_D})K_1(\sqrt{s+\bar{q}_D})+C_D s\left\{K_o(\sqrt{s+\bar{q}_D})+S(\sqrt{s+\bar{q}_D})K_1(\sqrt{s+\bar{q}_D})\right\}\right]} \tag{28}$$

where $\bar{q}_D = \dfrac{\gamma^2 m \tanh(m)}{1 + s_f m \tanh(m)}$ for slab shaped blocks

The parameters m, τ, and γ, are defined as,

$$m = \frac{\sqrt{\tau s}}{\gamma}; \quad \tau = \frac{h\phi_m c_m}{b_f \phi_f c_f}; \quad \gamma^2 = \left(\frac{2r_w}{h}\right)^2 \cdot \frac{k_m}{k_f} \cdot \frac{h}{b_f} \tag{29}$$

and are related to the Warren and Root parameters by,

$$\lambda^2 = \frac{\gamma^2}{s_f}; \qquad s_F = \frac{k_m b s}{k_s b_m} \tag{30}$$

and τ is the inverse of ω with the block system compressibility being negligible compared to the fracture system compressibility, and the block system thickness (average fracture spacing), fracture width and reservoir thickness included.

Equation 23 is solved by numerical inversion of the Laplace transform, in the double porosity solution of pressure transient data.

4.6 Type curve match

As has been shown above, combining boundary conditions of wellbore storage, skin, influence of fractures, bounded reservoirs and other reservoir and well boundary conditions, no simple solution of the radial diffussivity equation exists and various analytical and numerical solutions have been presented. For a single well in an infinite system with wellbore storage and thin skin Agarwal et al (1970), presented the solution in the form of type curves of for P_D vs t_D for various values of C_D and s. For a well of finite skin affected zone (composite reservoir) Watenbarger and Ramey (1970), presented another set of type

curves for various values of dimensionless wellbore storage and skin radius. Type curves for infinite conductivity and uniform flux vertical fractures, reservoirs bounded by linear faults, leaky aquifers and more recently for double porosity systems, have been presented and can be used to estimate reservoir properties. For more detailed treatment of this subject see Earlougher (1977).

For the infinite acting reservoir with wellbore storage and skin (type curves), a plot of the change in pressure with time, on the same scale as the standard type curve of Agarwal et al presented in Earlougher (1977) can be used to estimate reservoir and well properties. The principle is to select a match point and solve the equations for reservoir and well properties from the definitions of the dimensionless parameters.

$$T = \frac{kh}{\mu} = \frac{q}{2\pi}\left(\frac{P_D}{\Delta P}\right) \text{ match}$$

$$S = \phi c_t h = \frac{T}{r^2}\left(\frac{\Delta t}{t_D}\right) \text{ match} \qquad (31)$$

The dimensionless wellbore storage coefficient C_D and the skin factor s are obtained from the match curve.

5 APPLICATION OF WELL TEST ANALYSIS METHODS TO OLKARIA WELLS

5.1 Fall-off tests

The fall-off steps of wells 101, 201, 401, and 501 were analysed using type curve match, MDH and Horner methods. The fall-off steps were also analysed by computer, using analytical models for an infinite reservoir with skin and wellbore storage, the uniform flux vertical fracture without wellbore storage and the double porosity slab shaped blocks analytical model, with wellbore storage,skin and fracture skin. No good fit was obtained with the uniform flux vertical fracture model.

The analytical models have been used in the analysis of recovery data from Krafla wells by Sigurdsson et al (1985), which showed good fits to measured data, but gave generally lower transmissivities than initially estimated from injection tests at well completion. Double porosity systems have also been used in the interpretation of interference tests at Ngahwa geothermal field in New Zealand in which it was found that reservoir response to production/injection was better modelled with a double porosity system than with the infinite acting system, McGuiness (1984).

In the analytical fit to the infinite acting reservoir solution, initial guessed values of transmissivity T, formation storage S, skin s and dimensionless wellbore storage coefficient C_D from the infinite acting reservoir type curve match were used. The programme then adjusted these values to obtain the best fit to the measured data in a series of iteration steps. Because the initial pressure prior to the fall-off step was known, its value was kept fixed during the iteration steps. For most of the wells the programme required 10-15 iterations to obtain the best fit to measured data.

In the analytical fit to the double porosity system initial guess values of T, S, s, and C_D from the infinite acting reservoir type curves were used, with values of τ = 100, γ = 1E-4 and s_f = 0.1 - 1.0 being used as initial guess.

The initial pressure was kept fixed at its known value. The programme required 10-20 iteration steps to obtain the best fit to the measured data.

The results of the analyses are summarized in Tables 2 to 6. An example of the application of the different methods of analysis is given below for the fall-off at 1300 m in well 501, followed by a summary of the results for the other Olkaria wells. The data for well 501 is chosen because the longest fall-off steps were conducted in this well and the well does not recover rapidly in temperature above 1400 m, so thermal recovery effects are not significant. The well has only one major aquifer and so pressure control is at only one location.

5.2 Well 501 fall-off at 1300 m

5.2.1 Type curve match

Fig. 2 shows the type curve match for infinite reservoir with skin and wellbore storage. The match point is:

$s = -5.0$; $C_D = 1E+05$; $P_D = 0.17$; $\Delta P = 1E+05$; $t_D = 8E+04$; $\Delta t = 1E+02$.

The injection rate prior to the fall-off step was 27.67E-03 m3/s.

Transmissivity $$T = \frac{kh}{\mu} = \frac{q}{2\pi}\left(\frac{P_D}{\Delta P}\right) = \frac{27.67\times10^{-3}}{2\pi}\cdot\frac{0.17}{10^5}$$

$$T = 0.75\times10^{-8}\ \text{m3/Pas}$$

Storage $$S = \frac{T}{r^2}\left(\frac{\Delta t}{t_D}\right) = \frac{0.75\times10^{-8}}{(0.1082)^2}\cdot\frac{10^2}{8\times10^4} = 0.08\times10^{-8}\ \text{m/Pa}$$

From the available data good type curve match could not be obtained because the early time fall-off data is missing. From the initial pressure, the next recorded pressure during the fall-off step was after 7.4 minutes when the pressure had dropped by 8.1 bar. This is because the data have been collected mainly for analysis by semilog methods which do not require good knowledge of the early time

fall-off behaviour. The other reason is that the fall-off step was recorded downhole using a Kuster pressure instrument with 24 hour clock, from which it is not possible to read accurately times of less than one minute (1 minute = 3.5E-08 inches on 24 hour clock). The same applies to the fall-off step at 1400 m and the fall-off steps of wells 201 and 401.

5.2.2 Semilog analyses

a) MDH method

The MDH plot of the fall-off step at 1300 m is shown in Fig. 3. From the type curve match the time to expect the semilog straight line is given by:

$$t_D > 50 C_De^{0.14s} \quad \text{or} \quad t > 50 \frac{Sr_w^2}{T} C_De^{0.14s} \rightarrow t > 3089 \text{ sec}$$

Therefore we select a straight line after 3100 sec from which we obtain a slope of m = 4.3 bar/cycle.

$$\text{Transmissivity } T = \frac{kh}{\mu} = 0.1832\frac{q}{m} = \frac{0.1832 \times 27.67 \times 10^{-3}}{4.3 \times 10^5}$$

$$T = 1.18 \times 10^{-8} \text{ m3/Pas}$$

b) Horner method

Horner plot of the fall-off step (also shown in Fig. 3) yields a slope of 6.4 bar/cycle from which we obtain transmissivity of 0.79E-08 m3/Pas.

5.2.3 Computer fits to analytical models

Fig. 4 shows the best fit obtained with the model for infinite acting system using this approach. The computer printout of the measured data is shown in Table 8, while the calculated data is shown in Table 9. The data were

fitted to within 0.22% of the measured data with the following reservoir and well parameters, which shows fairly good agreement with the results of the hand fit above.

P_i = 106.4 bar (fixed); T = 0.99E-08 m^3/Pas; S = 0.18E-08 m/Pa; s = -3.5; C_D = 7.0E+04.

Fig. 5 shows the best fit obtained using the double porosity model, with the computer printout of the calculated data shown in Table 10. The data were fitted to within 0.04% of the measured data using the following well and reservoir properties.

P = 106.4 bar (fixed); T = 0.69E-08 m^3/Pas; S = 0.16E-08 m/Pa; s = -4.6; C_D = 6.0E+04; τ = 103; γ = 2.73E-04; s_f = .62.

It is not possible to indepedently determine the actual values of S, s, and C_D, by monitoring pressure changes in the disturbance well, because they are interrelated. To determine good values of S it is necessary to conduct interference tests. However, all fits used on well 501 consistently indicated a negative skin factor, indicating the influence of the fracture intercepted at 1390 m and hence the very good fit obtained using the double porosity model.

5.3 Summary of fall-off tests

a) Well 101

The results of the analyses are summarized in Table 2. The fits with analytical models are shown in Fig. 6 and 7. Because of the very short duration of this fall-off step, the exponential intergral type curve match and the analytical models do not give very reliable estimates of C_D, S, and s. The data could be fitted to a range of C_D from 1E+2 to 1E+4 and s from -3 to 0, with similar accuracy. However, both analytical infinite acting and double porosity models gave average transmissivity of 4.8E-08 m**3/Pas, with the type curve fit giving a higher value of 8.0E-08 m**3/Pas. Both MDH and Horner methods (Table 7) give lower values,

mainly because no sufficient time was allowed for the fall-off step. The analytical fits of within 0.05% of the measured data was obtained using both the infinite acting and the double porosity models.

b) Well 201

The results of the analyses are summarized in Table 3. The fits with the analytical models are shown in Fig. 8 to 9. The best type curve match indicates a very large positive skin, with high wellbore storage and a transmissivity of 4.0E-8 m^3/Pas, which could not be fitted to the analytical models. The analytical fits give an average transmissivity of 2.3E-08 m^3/Pas, and require a positive skin of about 10 for good fits. The double porosity fit indicates large matrix storage, large fracture permeability with no restriction to flow in the fractures. The results could also be influenced by the fact that pressure was monitored far below the major pressure control point and by thermal recovery. The semilog methods (Table 7) give similar estimates for the transmissivity as inferred by the other methods.

c) Well 301

As has been observed in the summary of well data, this well has a very high gas content (about 3.4 % in total discharge (KPC 1985)), with average temperature of less than 240°C over most of the permeable interval. This high gas content results in two phase conditions between casing shoe and 800 m, hence the ability of the well to discharge within a few hours after cold water injection.

The fall-off step conducted in this well exhibits typical composite reservoir behaviour caused by thermal recovery within the two phase zone. During the fall-off step, pressure drops for six minutes, stays almost stationary for a further eight minutes before dropping again. After 42 minutes when the fall-off step ended the pressure was far from stable (Fig. 10). This behaviour of well 301 is similar to that investigated by Garg and Pritchett (1981),

using a one dimensional vertical computer model to investigate the effects of cold water injection into a two phase reservoir. It was found that early time of the fall-off step was dominated by condensation effects, with the condensation front acting like a constant pressure boundary. At intermediate times, the condensation front begins to move towards the well (constant pressure period). The late time response is controlled by two phase conditions. In their analysis it was concluded that it is not possible to obtain absolute values of permeability from fall-off steps in two phase reservoirs. The value of the permeablity in this case can be obtained from the injection step. However, like for all Olkaria wells transient injection tests have not been recorded. Therefore the fall-off step of well 301 cannot be used to infer reservoir permeability.

d) Well 401

Two fall-off steps were conducted on this well, the first being at 1100 m after continuous water injection for over 20 hours. The fall-off step at 1100 m lasted nearly two hours. The results of the analyses at this depth are summarized in Table 5. The fits with analytical models are shown in Fig. 11 and 12. The type curve match indicates a high wellbore storage, a skin of +5 and a transmissivity of 4.3E-08 m^3/Pas. The infinite acting analytical model indicates lower transmissivity of 2.4E-08 m^3/Pas. The double porosity model indicates very high fracture permeability compared to the matrix, restricted fluid flow to the fractures and a transmissivity of 1.8E-08 m^3/Pas. Both semilog methods (Table 7) grossly underestimate the transmissivity as no true semilog straight line developes. This prompted a repeat of the injection and fall-off steps one week after completion tests, with the test being conducted at 1000 m and the fall-off step lasting 130 minutes. The results of the analyses at this depth are also summarized in Table 5 Fig. 13 and 14 show the fits with analytical models, which give similar values of transmissivity, wellbore storage and skin, with that obtained from the type curve match. The double porosity fit indicates large matrix storage, with smaller fracture permeability and less restricted fracture flow compared with the test

performed at 1100 m. The positive skin indicated in both of these tests is consistent with the fact that a permeable zone is cased off just above the casing shoe. The semilog methods (Table 7) give a fairly good estimate of the transmissivity inferred by the other methods.

e) Well 501

Data from the fall-off step at 1300 m, has already been presented above. The fall-off step at 1400 m preceded the one at 1300 m and was conducted after continuous injection for 13.5 hours, the fall-off step lasting 5 hours. The results of the analyses at this depth are also summarized in Table 6. The analytical fits are shown in Fig. 15 and 16. The results show generally lower transmissivity than in the test conducted later at 1300 m. The semilog methods (Table 7), give similar results to that obtained from the type curve and the analytical fits.

5.4 Recovery tests

The recovery tests of wells 101 and 201 following discharge were analysed using the infinite resevoir type curve match, semilog and the analytical infinite acting and doulble porosity models. It was generally found that because of the initial two phase conditions around the well, the early time response could not be accurately fitted with either the type curve match or the analytical infinite acting or double porosity models. In the analytical models, the same iteration procedure to that used in the fall-off tests was used. Because no good type curve match was obtained, initial guess values of transmissivity were obtained from the semilog methods with initial guess values of C_D, S, and s from the fall-off steps analyses. Similar guess values of τ, γ and s_f as for the fall-off steps were used in the double porosity fits. The programme required 10-20 iteration steps to obtain the best fit to the measured data. The results are summarized below.

a) Well 101

Pressure recovery of this well was monitored both at the wellhead and at 1000 m, following 387 days of discharge. Only data at 1000 m is considered for analysis, because wellhead recovery does not give true representation of total pressure recovery in the well below the water level.

The discharge produced a drawdown of 30 bara at 1000 m and pressure recovers very rapidly to stabilized values indicating a very small radius of influence and high permeability away from the well face. Estimation of the transmissivity assumming a radius of influence of 50 m yields a value of 0.5E-08 m3/Pas.

The pressure recovery is influenced by thermal recovery and condensation in the the two phase zone. The pressure at which single phase conditions should exist in the well depends both on the reservoir temperature and and the gas content of the reservoir fluid. The total gas content of the discharge fluid of well 101 is 0.44% by mass (KPC 1985). If the reservoir temperature is 250°C , then the partial pressure of CO_2 is given by Sutton (1976), as:

$$n = a(T)Pc,$$

where n = mass concentration of CO_2

P_c = partial pressure of CO_2 (Pa)

$a(T) = (5.4 - 3.5T/100 + 1.2\ (T/100)^2)E-09$

Using the gas concentration above we obtain a gas partial pressure of 10.6 bar. The minimum pressure for single phase conditions to exist is the sum of the saturation pressure at 250°C and the gas partial pressure. For this well this becomes 50.4 bara. Thus the pressure recovery of this well is completely masked by two phase conditions for the first two hours followed by near stabilized conditions. Because of these two phase conditions a fit with the infinite acting type curve or analytical models could not be obtained.

The large pressure drop close to the wellbore is probably caused by scale deposits (mainly calcite), in the formation around the well due to the high CO_2 content of the fluid. A similar interpretation was presented by Petty (1983), in the analysis of the effect of scaling on pressure transient data, which shows that erroneous results will be obtained if reservoir properties are calculated from the drawdown data, hence the small value of transmissivity calculated from the well productivity index using a drawdown of 30 bar.

Riney and Garg (1981) analysed the pressure transient behavior of well Baca 4, in which the effect of CO_2 is considered. Their analysis shows that semilog methods can be used after single phase conditions exist in the well. Using this method on the recovery data of well 101 both semilog methods (Fig. 17 and 18) yield a slope of 0.2 bar/cycle from which we calculate a transmissivity of 17.9E-08 m^3/Pas. This value is much higher than that obtained from the injection tests. These results are also summarized in Table 2.

b) Well 201

Pressure recovery of this well was monitored at 1000 m, following 281 days of discharge. The discharge produced a drawdown of 13.0 bar at this depth and a similar analysis to that of well 101 yields a transmissivity of 5.0E-08 m3/Pas.

The pressure recovery is slightly influenced by thermal recovery and gas content of the discharge. The well has about 0.07% gas by mass, with a reservoir temperature of about 240°C. The gas partial pressure is 1.8 bar. Therefore, single phase conditions should exist at 36.3 bara, which occurs after only 20 minutes of shut in.

Thus for this well both the type curve match and the analytical infinite acting and double porosity methods were used. No good fit was obtained using the type curve match and the analytical infinite acting model. Fig. 19 shows the fit obtained with the analytical double porosity model.

Because of apparent fluctuation in later time recovery only data up to 17 days of shut in were used. The double porosity fit indicates a high transmissivity of 11.2E-08 m3/Pas with apparently large skin caused by two phase conditions existing around the well prior to shut in. The fit also indicates large wellbore and matrix storage and relatively high fracture permeability, with no restriction to fluid flow in the fractures.

The MDH and Horner methods (Fig. 20), both yield a slope of 0.5 bar/cycle from which, we calculate a transmissivity of 16.4E-08 m3/Pas, which is much higher than that obtained during the injection tests. These results are also summarized in Table 3.

5.5 Analysis of well injectivity

Values of well injectivity from the step injection tests of wells 101 to 501 have already been presented in the summary of well data. This injectivity is obtained by measuring the static rise in pressure at each pump rate during the step injection test. For Olkaria wells injectivity has generally been found to increase with injection rate and also with the duration of pumping. Thus to obtain reliable values of injectivity it is necessary to conduct injection steps of long enough duration to eliminate wellbore storage effects.

The value of the well injectivity obtained during cold water injection into a hot water reservoir is a non-isothermal value but can be related to the isothermal injectivity index, and be used to inferr well poductivity and transmissivity as long as the radius of the cold spot can be evaluated, and the apparent viscosity obtained, Sigurdsson et al (1983).

Because of the increase in injectivity with injection rate and the fact that injection steps of short duration were used on most of the wells, no reliable estimates of transmissivity are possible from these values of injectivity. However since these are the only values

available for estimation of the transmissivity of well 301, an estimate of transmissivity is obtained by assuming an effective radius:

$$T = \frac{2.303 II}{2\pi} \log\left(\frac{r_e}{r_w}\right)$$ II = Non isothermal injectivity index

The value of r_e assumed does not make a large error once the log term is taken and we use a r_e = 50 m. The values of transmissivity obtained from this estimate are summarized in Tables 2 to 6, in which it is found that generally higher estimates than obtained from the transient tests are obtained. From this estimate the transmissivity of well 301 is found to be higher than 4.8E-08 m3/Pas.

5.6 Reservoir permeability

The table below summarizes the values of reservoir transmissivity obtained for the Olkaria West field together with the permeability thickness product and the absolute permeability of the reservoir assuming the reservoir extends over the interval in which permeability was encoutered in the well.

WELL NO.	TRANSMISSIVITY m3/Pas E-08	TEMPERATURE C°	THICKNESS m	kh d-m	k md
a. FALL-OFF TESTS					
101	5.0	250	1000	5.5	5.5
201	2.2	240	500	2.5	5.0
301	>4.8 ?	250	1000	5.3	5.3
401	2.2	240	1000	2.8	2.8
501	0.85	250	500	0.93	1.9
b. RECOVERY TESTS					
101	17.9	250	1000	19.5	19.5
201	14.0	240	500	15.8	31.6

In calculating the kh for the reservoir using the fall-off steps, the value of hot water viscosity is used. This is consistent with the results of Cox and Bodvarsson (1985), in their analysis of non isothermal injection tests in porous and fractured media.

In calculating the kh from the recovery tests, reservoir properties of saturated liquid are used, because two phase conditions in the well are only transitional lasting only 2 hours in well 101 and 20 minutes in well 201.

The fall-off steps indicate an average reservoir permeability in excess of 5.0 md for all the wells in which extensive fracture zones are encoutered. The smaller value indicated for well 401 is due to the casing off of a permeable zone at 800 m, while well 501 does not seem to intercept a large enough fractured zone.

Recovery following discharge, indicates much higher reservoir permeability, but these results have to be confirmed from the repeat tests as there was considerable scatter in the later time recovery data.

5.7 Comparison with Olkaria East

Table 1 summarizes the reservoir properties of the Olkaria East field from the initial well test analyses, history match and a reanalysis of the recovery tests and some fall-off tests by KRTA Ltd (KPC 1984b). The major conclusion from these data is that well tests performed on the Olkaria East wells generally do not give good indications of the reservoir properties. The fall-off tests generally over-estimate the transmissivity, because for most of the Olkaria East wells the injection steps lasted only 20 to 40 minutes followed by similar duration of fall-off step. Non isothermal effects and wellbore storage greatly influenced these results.

The recovery tests of Olkaria East wells on the other hand generally under-estimate the transmissivity mainly due to two phase transients predominating in these wells during

discharge, because the Olkaria East field shows saturated liquid conditions below the steam cap.

Comparison of the results obtained for Olkaria West with those of the history match of Olkaria East wells, shows that the reservoir permeability of Olkaria West wells intercepting fractures compares with that indicated for the best wells in Olkaria East. However, larger outputs should be expected from the Olkaria West wells because of the low discharge enthalpy of these wells.

5.8 Recommendations for future testing

In order to obtain reliable estimates of the reservoir transmissivity the following testing procedure should be adopted.

1. Well testing should start immediately after drilling is completed, without allowing the well to recover in temperature, in order to minimize the effects of thermal recovery. At present the wells are allowed to recover in temperature for periods of over two days in order to perform water loss tests, for identification of permeable zones in the well. This is not necessary and permeable zones in the well should mainly be assessed from losses during drilling, temperature profiles during pumping and from temperature and pressure recovery during heating prior to discharge. In some of the wells, e.g well 401, completion tests have been delayed for several days in order to perform water loss tests.

2. During injection tests pressure instruments should be kept at a fixed depth throughout the duration of the injection and fall-off steps in order to measure accurately the small pressure changes. Moving the intruments during tests introduces errors due to hysteresis in pressure recorders and possible depth discrepancy wich can affect the small pressure changes.

3. At present only the transient pressure fall-off steps are analysed. The transient pressure injection steps should also be recorded and analysed in similar manner.

4. Quite often the early time data are missing from the fall-off step records. Where possible these should be read from the downhole pressure recorder charts and used to check the values of the reservoir and well properties obtained in the analyses presented in this report. With the acquisition of surface recording equipment, more accurate records of pressure from the injection and fall-off steps should be possible.

5. Fall-off steps conducted in well 501 indicate that wellbore storage effects last in excess of one hour. Therefore in order to minimize the effects of wellbore storage, fall-off steps of at least 3 hours each should be used, with similar duration of injection steps. The actual values of optimum injection fall-off step duration will vary from well to well and should be estimated with a short fall-off step of about 1-1.5 hours prior to the start of the step injection test. The duration of the tests can also be designed based on field experience and knowledge of zones cut by drilling.

6. Pressure recovery data show considerable scatter some of which could be due to instrument error and the fact that excessive pressure leakage occured during the recovery runs in which whole well profiles were taken. Pressure leakage during the runs should be minimized by using sealing glands and good wellhead valves. For the purposes of pressure recovery at a selected depth, spot recovery runs should be taken at this depth, which will minimize the disturbance in pressure profile caused by excessive pressure leakage.

7. Interference tests should be carried out for evaluating reservoir properties and boundary effects over a larger area. Recent interference tests at Ngahwa and Ohaaki geothermal fields in New Zealand (McGuiness, 1984) show that response to prodution/injection is observed within one hour at a distance of 2 km.

8. Every effort should be made to measure well outputs accurately, if necessary using pressure separators, as analysis of transient pressure recovery tests critically depends on measured values of mass output and enthalpy.

6 GENERATING CAPACITY

6.1 Stored heat assessment

KPC (1984b) gives a stored heat assessment of the Olkaria geothermal resource. The reservoir capacity is obtained by using the following reservoir parameters for the entire resource area.

Porosity 0.12; Rock density 2680 kg/m3; Rock specific heat capacity 820 J/kg°C; Water density 830 kg/m3; Water specific heat capacity 4.75 KJ/kg°C; Thermal recovery factor 0.5; Conversion efficiency 0.15.

The following temperature distribution is assumed:

Depth (m)	Temperature (°C)
500	200
800	250
900	260
1150	280
1400	300
1900	330

Using these reservoir parameters, the following generating capacity is obtained:

Depth interval (m)	Average temp (°C)	Thermal capacity PJ/km^2	Electrical capacity MW yr/km^2	Sustainable output for 25 years MWe/km^2
500 - 800	225	14.5	35	1.4
800 - 900	255	13.2	31	1.2
900 -1400	280	96.2	229	9.2
1400-1900	315	138.4	329	13.2
Total			624	25.0

Using an aerial extent of 100 km^2 as defined by the low resistivity boundary, it is apparent that the Olkaria geothermal field constitutes a substantial resource of about 2500 MWe for 25 years, but 90% of this energy resource is in the depth interval 900-1900 meters.

6.2 Reservoir depletion study

6.2.1 Model used

In order to study the depletion process of the entire Olkaria reservoir, without confining the study to Olkaria East as was done in KPC 1984a, a three dimensional three layer model shown in Fig. 21 and 22 was used, with the field divided into five areas along the existing faults and fractures. Because 90% of the energy is below 900 meters, a one km thick caprock was used, with the reservoir extending to a depth of 2 km. The initial temperature and pressure distribution and the horizontal permeability for these five areas is summarized below:

Area Location	Average temp	Average pressure Bar (a)	Total area km^2	Horinzontal permeability md
1 Olkaria East (A-1)	282	0.2(b)	25.0	8.0
2 Around well 501 (A-2)	280	100	17.0	8.0
3 Around wells 301 and 601 (A-3)	300	120	29.0	8.0
4 South of well 301 (A-4)	280	90	17.0	8.0
5 Between Olol-Butat and well 401 faults (A-5)	230	90	7.6	8.0
6 Olkaria fault	300	110	1.25	50.0
7 Olkaria 101 fracture	280	90	0.61	50.0
8 Olkaria 401 fault	230	90	0.61	50.0
9 Ololbutat fault	200	90	0.61	50.0

(a) Average pressure at depth of 1500 meters

(b) Average vapour saturation caused by current production, (from history match at the end of 1983).

The assumed temperature distribution for the reservoir area is the average as indicated by the drilled wells within the area. The value of horizontal permeability used in the reservoir areas is intermediate between that obtained from fall-off and recovery steps analyses for Olkaria West wells and also corresponds to that obtained from the history match for the best wells in Olkaria East. The faults are modelled as highly conductive channels with average width of 10 meters and extending to the reservoir bottom. Vertical permeability is assumed to be one tenth of horizontal permeability for all elements.

Each reservoir element has a single confining caprock element above at an average temperature of 150°C with permeability about one hundredth of that in the reservoir. An atmosphere at a constant temperature of 25°C is above the caprock. The entire reservoir is underlain by a single large element at a constant temperature of 320°C with permeability about one fifth of that in the reservoir. The atmosphere and the base elements are held at a constant temperature by specifying an artificially high specific heat capacity.

All internal boundaries are modelled as flow boundaries except for the boundary between Olkaria well 101 fracture and the Olkaria fault which is modelled as a no flow boundary. All outer boundaries are no flow boundaries (i.e. no recharge from the sides). Flow from the base element into the reservoir is allowed through the interconnecting faces. Relative permeabilities are assumed to be linear functions of vapour saturation in the producing elements and full gravity is modelled. For more details concerning the generation of connections and the computation procedure, refer to Shaft79 users manual (Pruess and Schroeder, 1980). The following reservoir properties are held constant throughout the simulation.

Porosity (faults) 0.05; Porosity (all other elements) 0.02; Rock density 2650 kg/m^3; Rock Specific heat capacity1,000 J/kg°C; Rock conducitivity 2.0 W/m^2°C; Residual immobile water saturation 0.35; Residual immobile steam saturation 0.05; Perfectly mobile steam saturation 0.55.

The value of reservoir porosity used corresponds to that used for the outer elements in the history match for Olkaria East.

6.2.2 Generation rate

Even if the Olkaria geothermal field constitutes a very large resource, development is likely to proceed in small stages, in line with power demand as has been the case for Olkaria East. Therefore, in order to study the depletion process with the very coarse model used, the following constant mass generation rates were used.

Area	Mass flow kg/s	Initial steam at 6 bar kg/s	Initial MWe (a)
1	170	59.0	23.0
2	200	54.0	21.7
3	200	64.6	25.9
4	200	54.0	21.7
5	300	46.2	18.6
Total	1070	277.8	110.9

(a) Using 2.5 kg/s steam per MWe

The mass output used for the Olkaria East corresponds to the current total mass output while generating 45 MWe. The difference in the equivalent power output from the one used in this study, is due to the fact that actual vapour saturation in the producing elements is much higher than the average value assumed for the single element representing this area and contribution from the steam zone being neglected by using a 1 km thick caprock.

Because the steam quality in the producing elements increases with time, imposition of a constant mass generation rate will result in an increase in steam proportion with time. The constant mass generation rates were thus selected with this constraint.

The simulation was initially carried out in three small time steps, beginning with a time step of 8.8 hours and increasing it by a factor of ten twice. A full simulation was then carried out for a period of 16 years, with production from all areas. Because thermodynamic properties in area 5 were out of range after 15 years as the area produced superheated steam, the simulation was repeated for thirty five years without production from this area. At 34.7 years the simulation was terminated as thermodynamic properties in area 4 also went out of range following its depletion.

6.2.3 Results of simulation

The results of the reservoir depletion study are summarized in Figs. 23 to 25 which show the variation in pressure, vapour saturation and production enthalpy in the five areas with time during the 35 year simulation period.

Pressure in all the producing elements (Fig. 23) quickly drops within the first few months of production and then declines slowly, as vapour saturation increases. Vapour saturation in area 5 reaches 100% in 15 years (Fig. 24) after which the pressure quickly drops as the reservoir is depleted. When no prodution is imposed on area 5, the pressure drops slowly to the saturation value in about seven years, and then slowly increases as the liquid begins to boil due to the heat supply from the base element, reaching a saturation of 15% after 35 years of production from the other areas.

Vapour saturation in area 4 reaches 100% at 33 years after which the pressure quickly drops as the area is depleted and would soon be followed by area 2 (where vapour saturation after 34.7 years is 98.5%), if a longer production period were used.

Production enthalpy in area 5 rises to 2800 KJ/kg after 9.5 years (Fig 25), as vapour saturation exceeds 65% and liquid mobility drops to zero. Pure steam production occurs after 19.5 years in area 4, 21 years in area 2, 21.5 years in

area 1 and 26.3 years in area 4. The total steam production at 30 years (no production from area 5) is equivalent to over 300 MWe and at the end of the simulation when area 4 is depleted, the production is equivalent to 230 MWe.

At the end of the 34.7 years simulation period, no considerable change has occurred in the temperature of the producing elements and the final condition is as follows:

Area	Temp (°C)	Vapour saturation (%)	Pressure Bar
1	278.5	85.4	62.9
2	274.5	98.7	59.6
3	297.0	78.8	82.4
4	274.5	100.0	7.7
5	230.7	15.1	28.3

Of the original fluid mass in the reservoir only 22% remains after 34.7 years of production, but of the original energy in place only 3% has been extracted because 98% of the energy is in the rock.

Boiling takes place in all the fault elements and after 34.7 years vapour saturation exceeds 64%, the highest being 86% for the Olkaria fault.

6.3 Discussion

From the stored heat assessment it is evident that the Olkaria geothermal field comprises a substantial resource, but the recoverable resource depends on the thermal recovery factor, which is very difficult to quantify. The recoverable energy also depends on the effective rock porosity which could be lower than the value used in this stored heat assessment.

From the simple model used in this depletion study, using an effective porosity of 2%, the Olkaria field can support an average of 250 MWe for 35 years, if no recharge takes place. This effective porosity corresponds to that used for the outer elements in the history match of production for Olkaria East. If the effective porosity is that low, then the depletion study shows that economical energy recovery will depend greatly on recharge to the system. Area 5 cannot be economically used for power generation because of the low temperature.

To this simple model, effects of recharge to the system, division of the reservoir area into smaller elements, varying thickness of the caprock, temperature variation with depth, and variation in permeability and porosity can be investigated. However, these were beyond the scope of this study.

ACKNOWLEDGEMENTS

It gives me great pleasure to express my gratitude to Omar Sigurdsson for the excellent guidance during the training period and for critically evaluating the work presented in this report.

I would also like to express my gratitude to Dr. Ingvar Birgir Fridleifsson, the staff of the UNU and the National Energy Authority of Iceland, for the excellent organisation of the training programme.

Special acknowledgements go to the management of the Kenya Power Company, the Government of Iceland and the UNU who enabled me to attend this very valuable course.

REFERENCES

1. Agarwal, R.G., Al-Hussainy, R. and Ramey, H.J. Jr (1970): An investigation of wellbore storage and skin effect in unsteady liquid flow, Analytical treatment. SPE Journal, Sept 1970.

2. Bodvarsson, G.S. et al (1984): Krafla geothermal field, Iceland. Analysis of well test data. Water resources research Vol 20, No. 11 (Nov 1984).

3. Cox, B.L. and Bodvarsson, G.S (1985): Nonisothermal injection tests in fractured reservoirs. 10th Workshop on Geothermal Rreservoir Eengineering, Stanford University (Jan 1985).

4. Da Prat, G. (1982): Well test analysis for naturally fractured reservoirs. 8th Workshop on Geothermal Reservoir Engineering, Stanford University (Dec 1982).

5. Earlougher, R. C. Jr. (1977): Advances in well test analysis. SPE Monogragh No 5 (1977).

6. Garg, S.K. and Pritchett, J.W. (1981): Cold water injection into two phase geothermal reservoirs. 7th Workshop on Geothermal Reservoir Engineering, Stanford University (Dec 1981).

7. Grant, M.A, et al (1982): Geothermal Reservoir Engineering. Academic Press (1982).

8. Gringarten, A.C., Ramey, H.J.Jr., and Raghaven, R (1974): Unsteady-state pressure distributions created by a well with a single infinite-conductivity vertical fracture, SPE Journal, aug, 1974.(1984). KRTA, Ltd.

9. Kjaran, S.P. and Elliasson, J. (1983): Geothermal reservoir engineering, lecture notes. UNU, Iceland (1983).

10. KPC,: Completion tests, heating, discharge and shut in tests of wells 101 and 201. (unpublished reports).

11. KPC,: Completion tests and heating of wells 301, 401, and 501. (unpublished reports).

12. KPC, (1980): Olkaria Geothermal field - Preliminary studies of the generating capacity by G.S. Bodvarsson (1980).

13. KPC: Completion tests and heating of wells 301, 401, and 501. (unpublished reports).

14. KPC, (1984a): History match and performance prediction for Olkaria Geothermal Field, by G.S. Bodvarsson.

15. KPC, (1984b): Background report for the STRM of Olkaria, KRTA Ltd.

16. KPC,(1984c): Recent measurements within Olkaria East and West fields . Report for Scientific and Technical review of Olkaria (1984). by Haukwa C.B. (unpublished report).

17. KPC, (1985): Steam status report (July 1985).

18. Lee, John (1982): Well Testing. SPE text book series 1982.

19. McGuinnes, M.J. (1984): Recent interference tests at Ngahwa and Ohaaki. Proceedings of the New Zealand geothermal workshop (1984)

20. Moench, A.F. (1983): Well test analysis in naturally fissured geothermal reservoirs with fracture skin. 9th Workshop on Geothermal Reservoir Engineering, Sanford University (Dec 1983).

21. Petty, S. (1983): Effects of scaling on downhole pressure transient data. 9th Workshop on Geothermal Reservoir Engineering, Stanford University (Dec 1983)

22. Pruess, K. and Schroeder R.C., (1980): Shaft79, user's mannual. LBL-10861. Lawrence Berkly laboratory. University of California.

23. Ramey, H.J. Jr, et al, (1981): Reservoir engineering assessment of Geothermal systems. DPE, Stanford University.

24. Reynolds, A.C, Raghavan, R., Elbel, J.L (1982): Performance of finite conductivity vertically fractured wells in a single layer reservoir. SPE Journal Sept 1982.

25. Riney, T.D and Garg, S.K (1981): Analysis of flow data from several Baca wells. 7th Workshop on Geothermal Reservoir Engineering, Stanford University (Dec 1981).

26. Sigurdsson, Omar et al (1983): Nonisothermal injection tests can infer well productivity and reservoir transmissivity. 9th Workshop on Geothermal Reservoir Engineering, Stanford University (Dec 1983).

27. Sigurdsson, Omar et al (1985): Pressure buildup monitoring of the Krafla geothermal field Iceland. 10th Workshop on GRE Stanford University (Jan 1985).

28. Sigurdsson, Omar (1985): Lecture notes for the UNU reservoir engineering course 1985 (unpublished).

29. Streltsova, T.D. and MacKnnley, R.M (1984): Effect of flow time duration on the build up pattern for reservoirs with hetrogenous properties, SPE Journal (June 1984).

30. Sutton, F.M (1976): Pressure-Temperature curves for a two phase mixture of water and carbon dioxide. New Zealand Journal of Science, 1976 vol 19.

31. Warren, J.E. and Root, P.J. (1963): The behavior of naturally fractured reservoirs. SPEJ, 245-255.

32. Waruingi, S.N. (1982): A Study of the Olkaria geothermal reservoir when generating thirty megawatts of electricity. Report No 82.22, Geothermal Institute, University of Auckland, New Zealand.

33. Wattenbarger, R.C, and Ramey, H.J. Jr (1970): An investigation of wellbore storage and skin effect in unsteady liquid flow, II.Finite difference treatment. SPE Journal, Sept 1970.

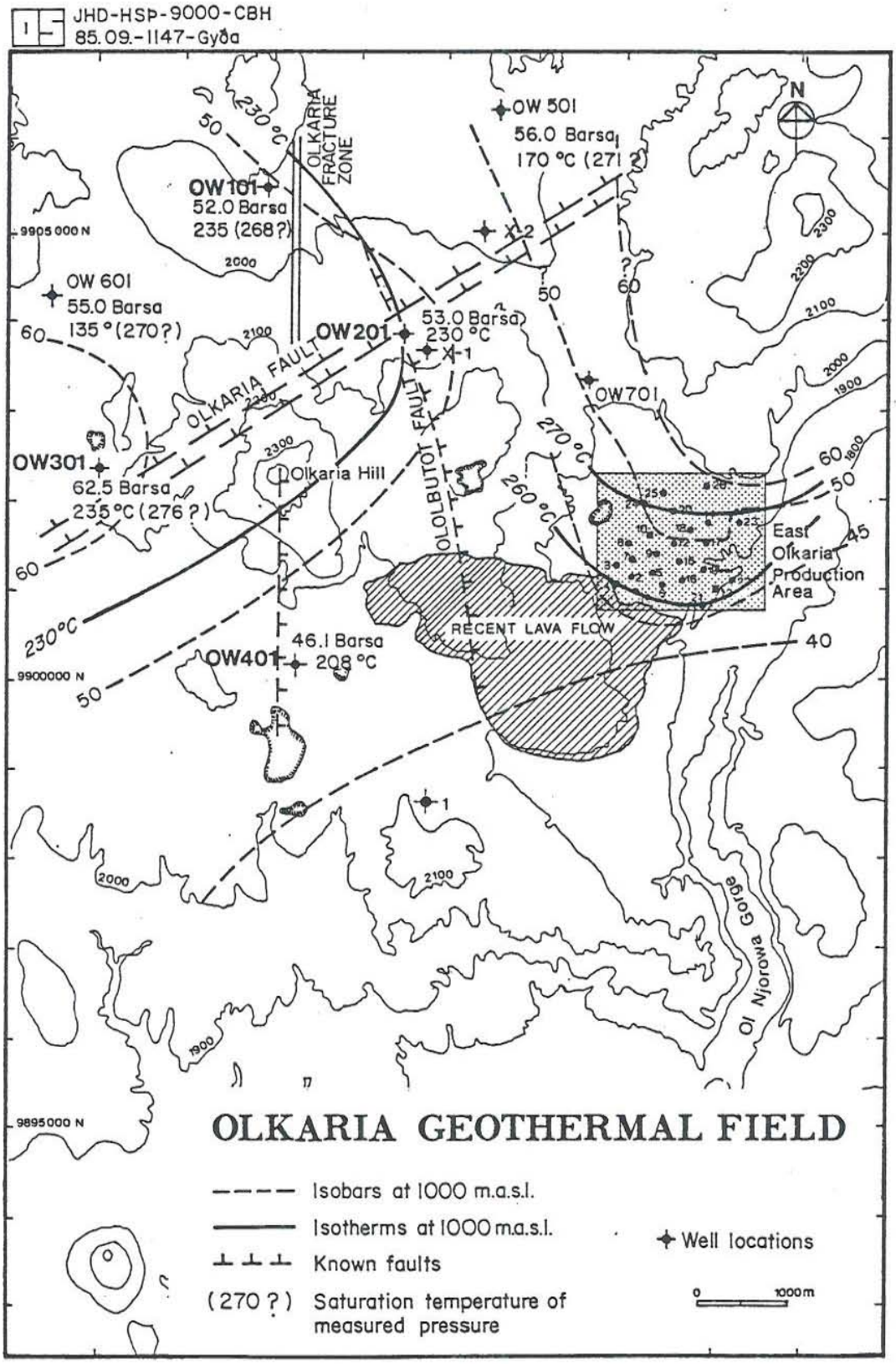

Fig. 1. Location of Olkaria geothermal field and temperature/ pressure distribution at 1000 masl.

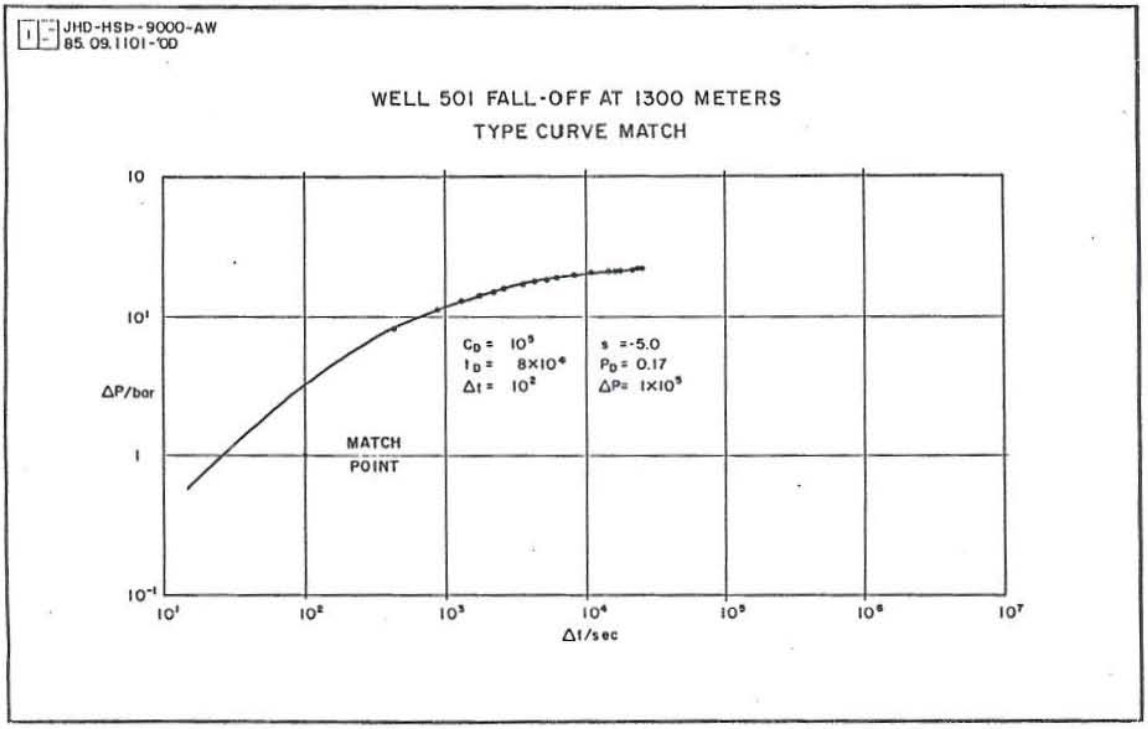

Fig. 2. Type curve match of pressure fall-off at 1300 m in well 501.

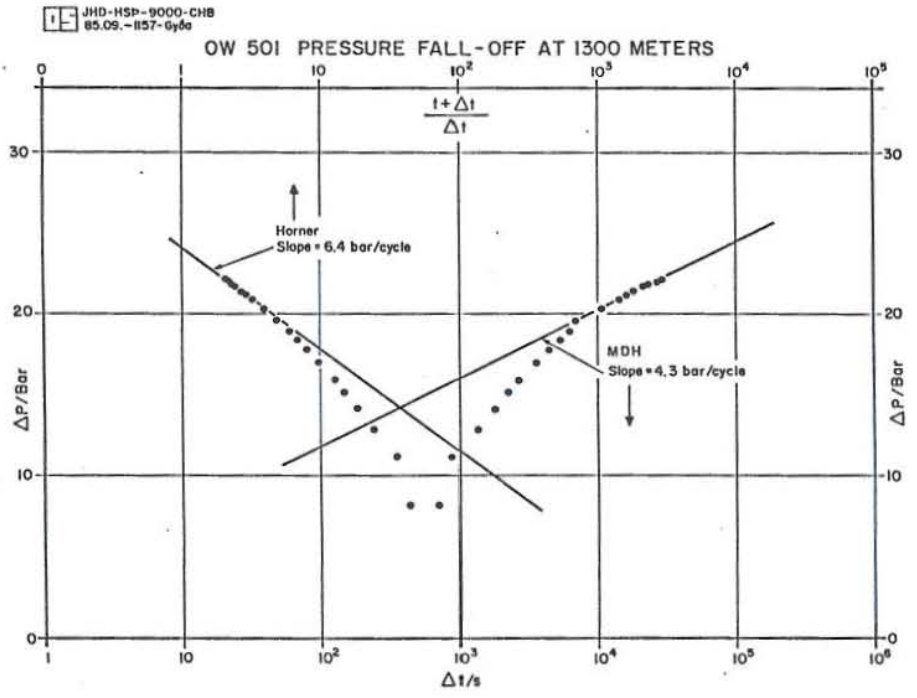

Fig. 3. Semilog plot of pressure fall-off at 1300 m in well 501.

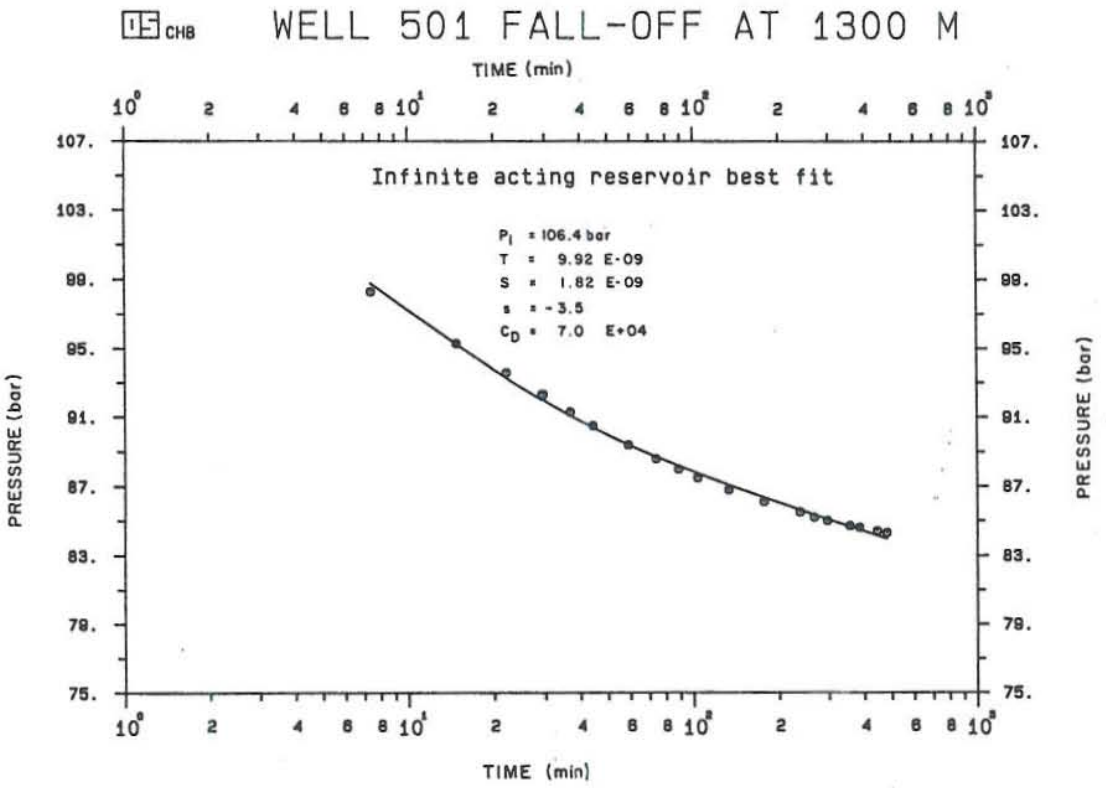

Fig. 4. Analytical infinite acting reservoir fit of pressure fall-off at 1300 m in well 501.

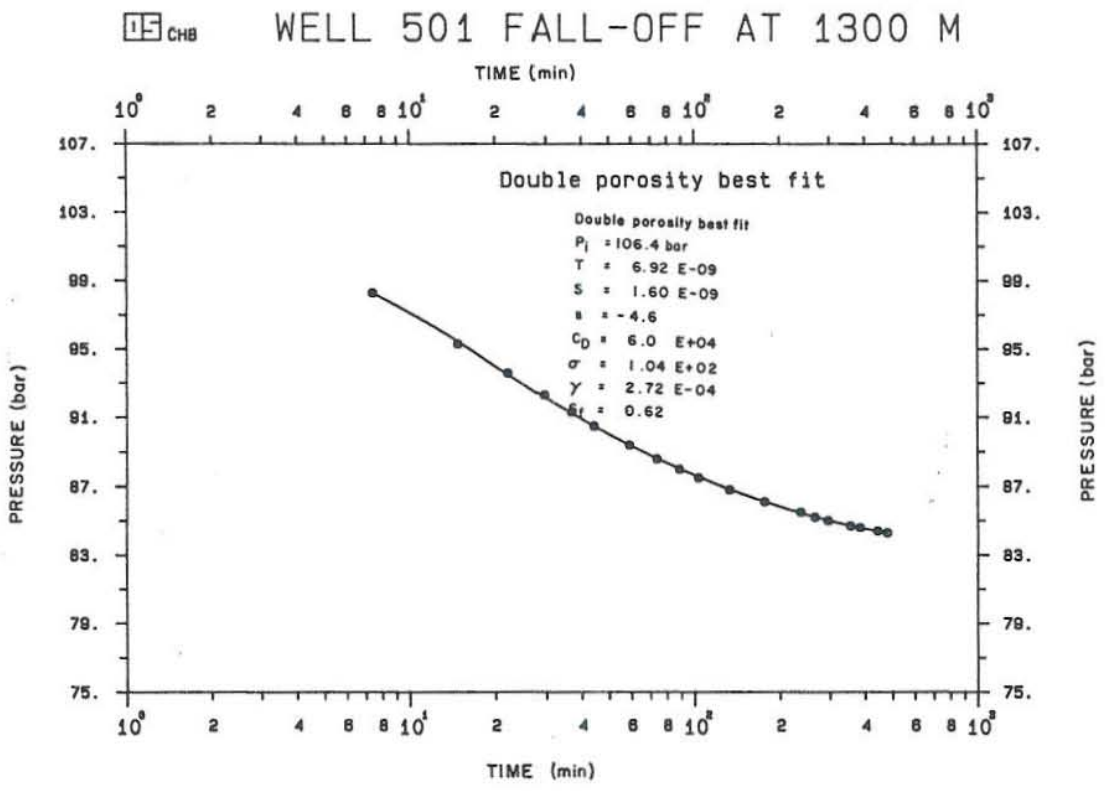

Fig. 5. Analytical double porosity fit of pressure fall-off at 1300 m in well 501.

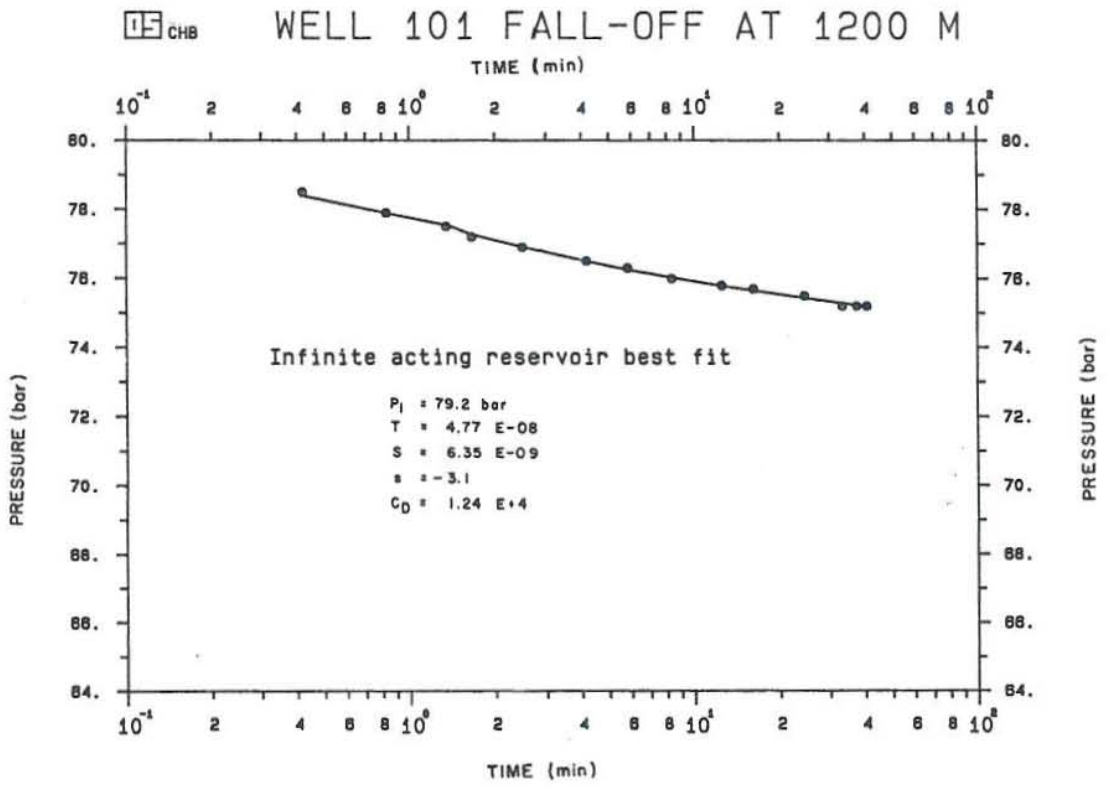

Fig. 6. Analytical infinite acting reservoir fit of pressure fall-off at 1200 m in well 101.

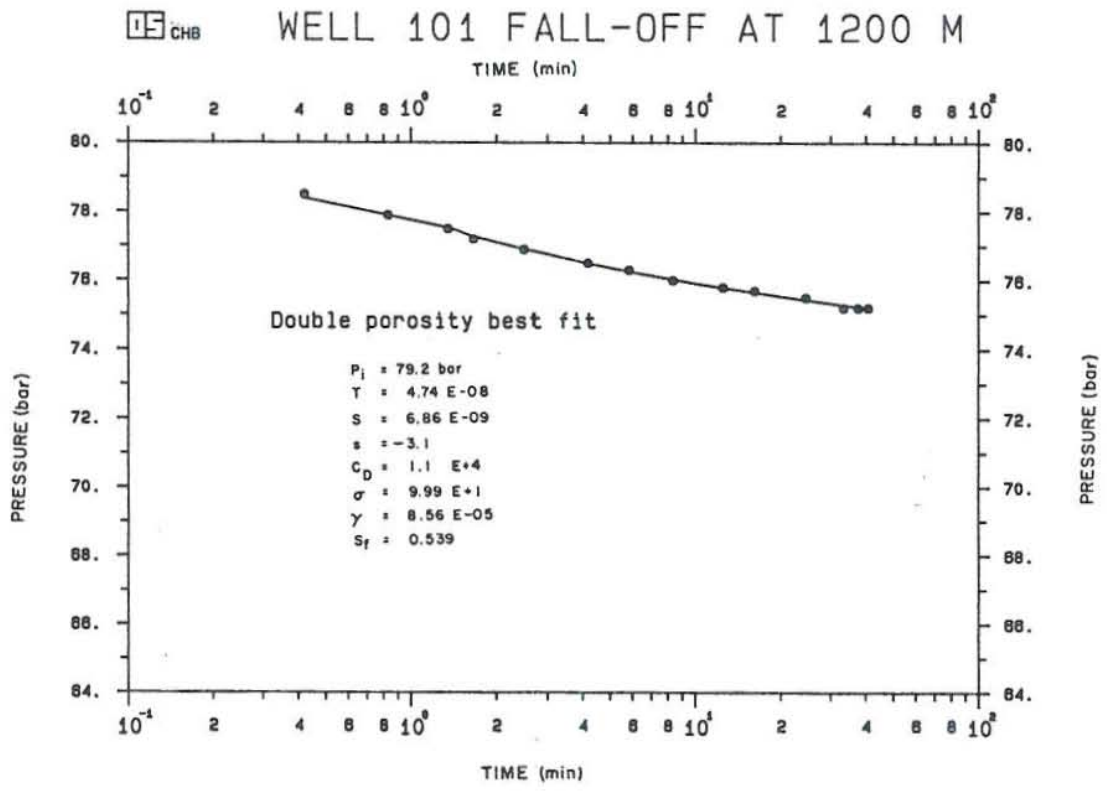

Fig. 7. Analytical double porosity fit of pressure fall-off at 1200 m in well 101.

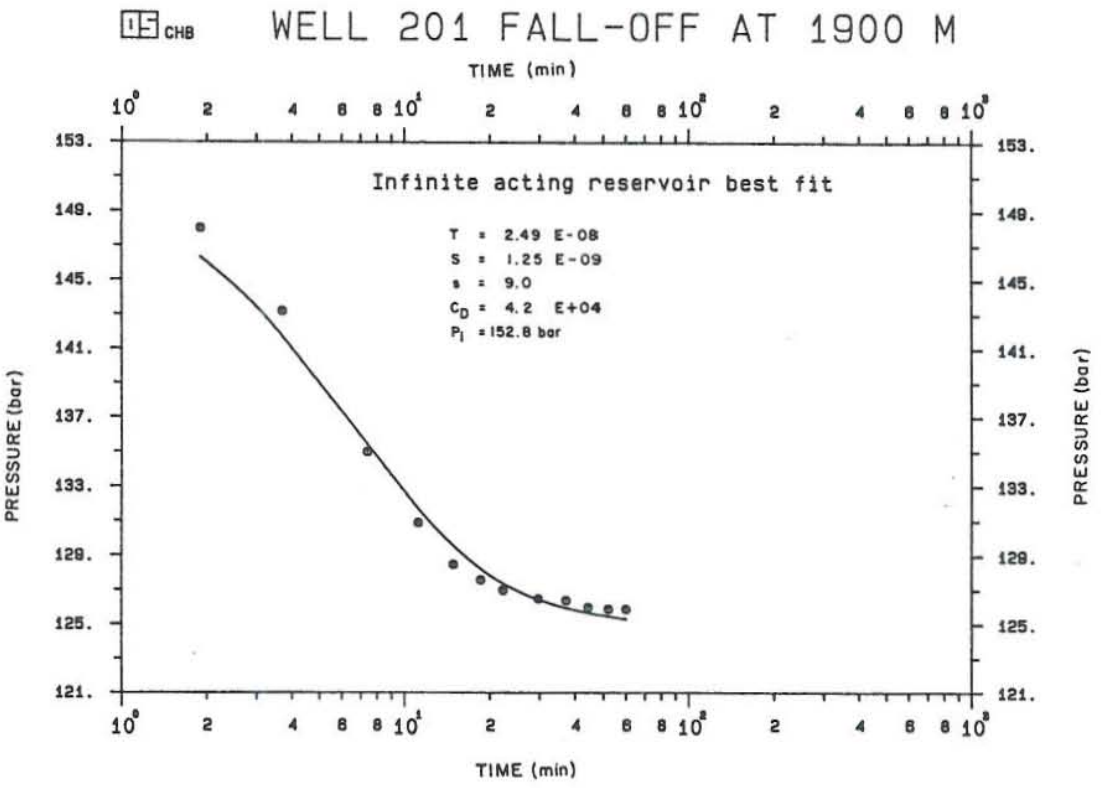

Fig. 8. Analytical infinite acting reservoir fit of pressure fall-off at 1900 m in well 201.

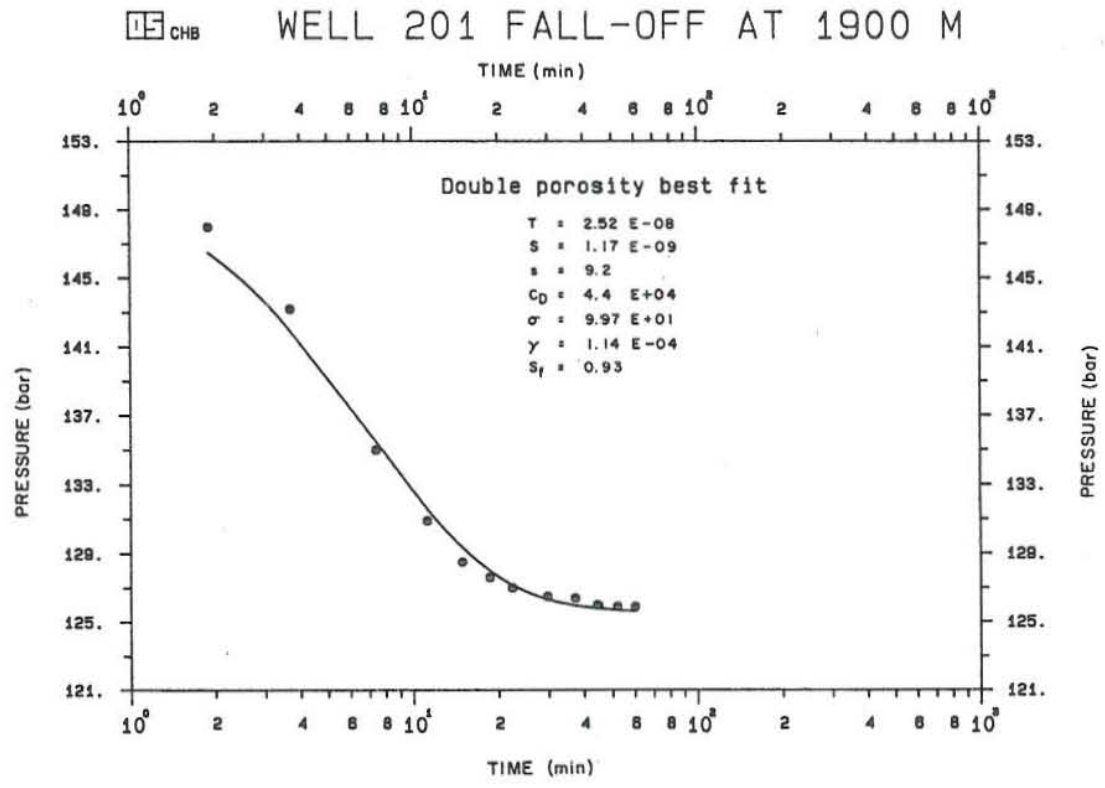

Fig. 9. Analytical double porosity fit of pressure fall-off at 1900 m in well 201.

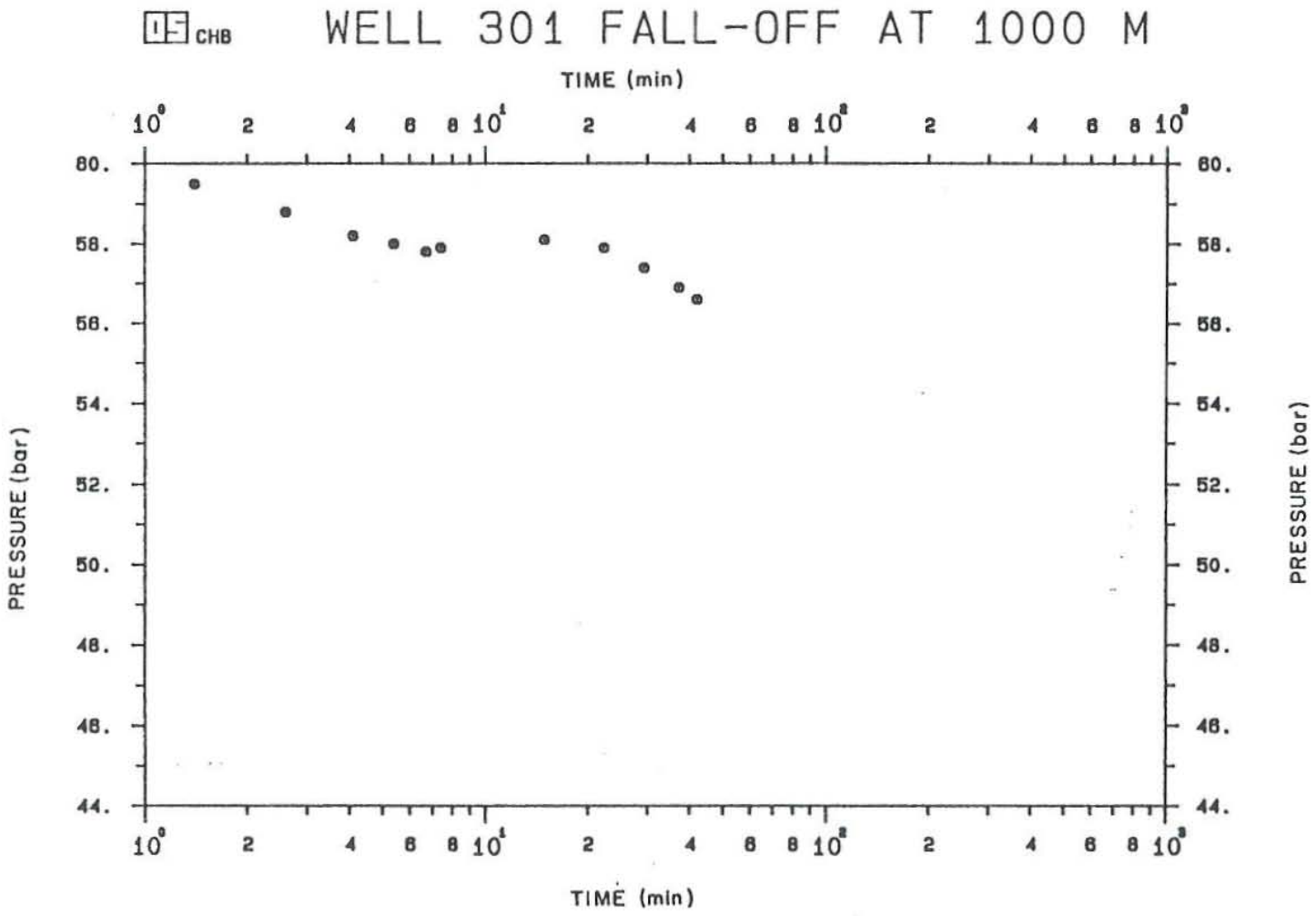

Fig. 10. Semilog plot of pressure fall-off at 1000 m in well 301.

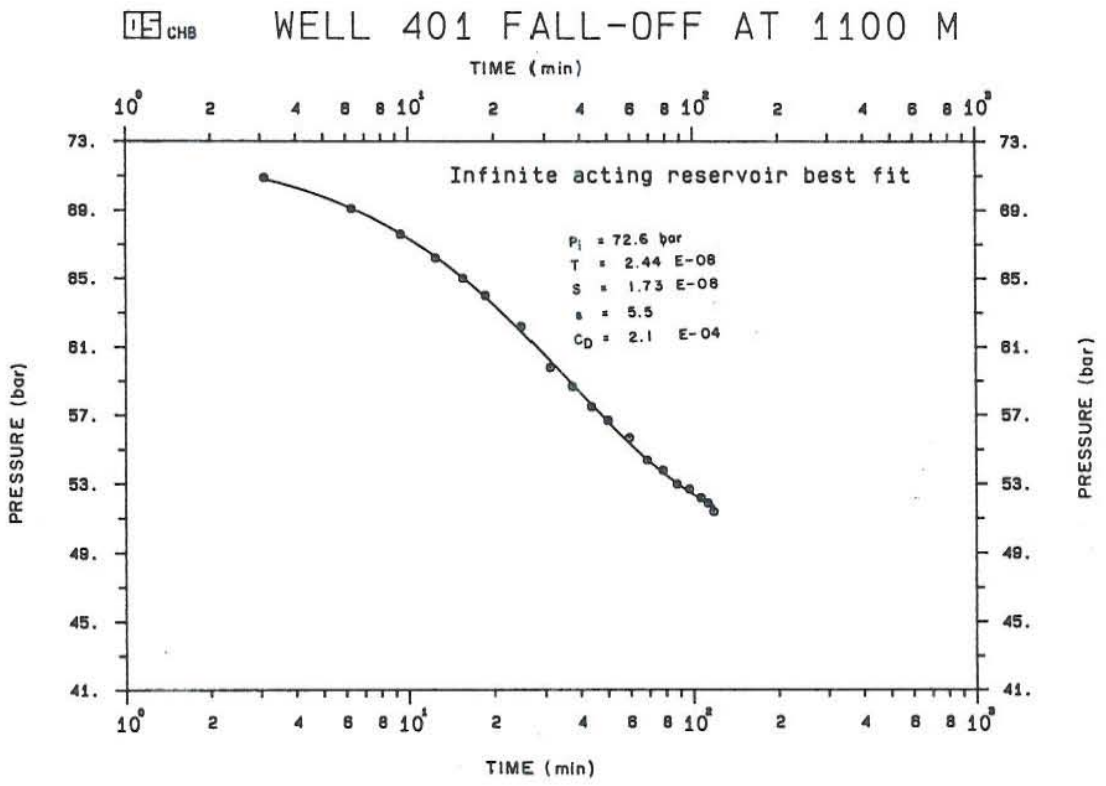

Fig. 11. Analytical infinite acting reservoir fit of pressure fall-off at 1100 m in well 401.

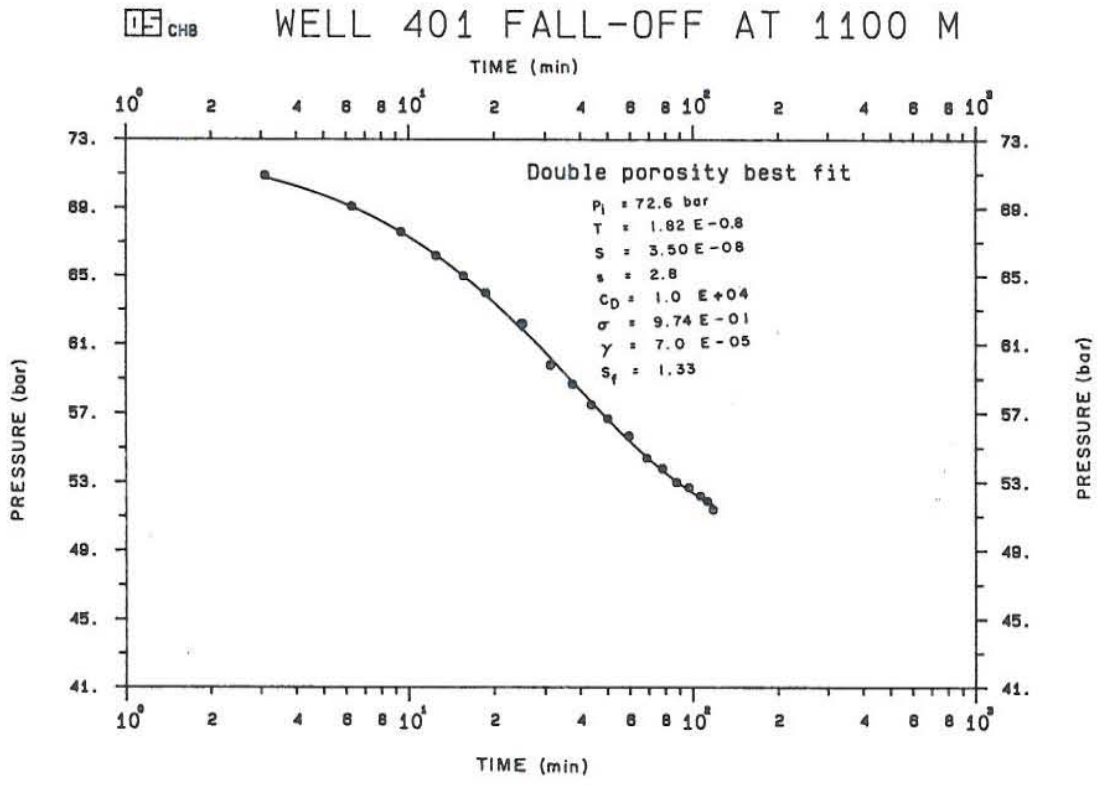

Fig. 12. Analytical double porosity fit of pressure fall-off at 1100 m in well 401.

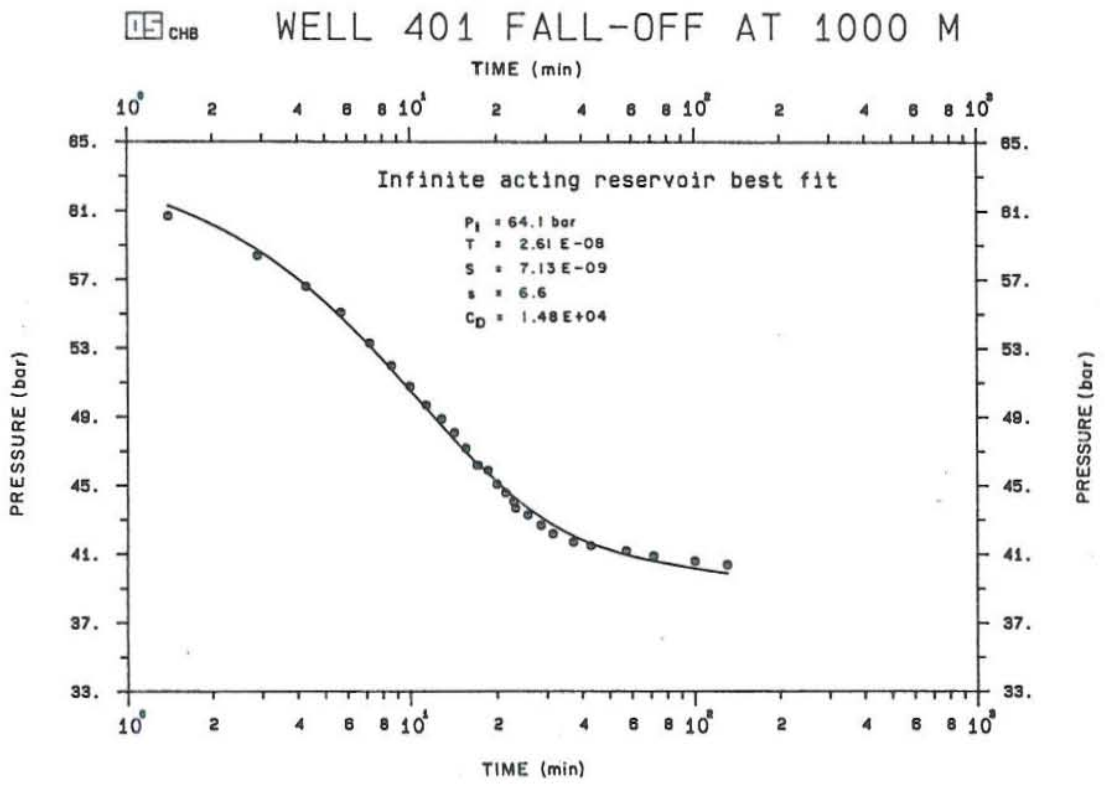

Fig. 13. Analytical infinite acting reservoir fit of pressure fall-off at 1000 m in well 401.

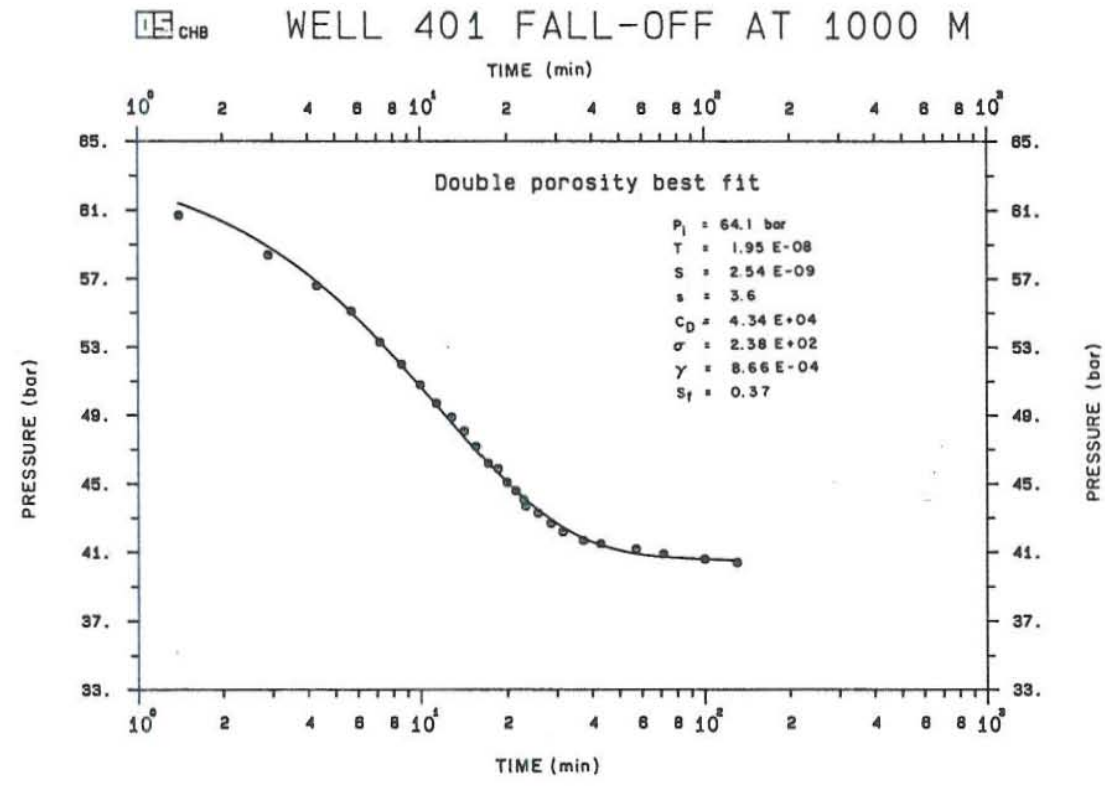

Fig. 14. Analytical double poorosity fit of pressure fall-off at 1000 m in well 401.

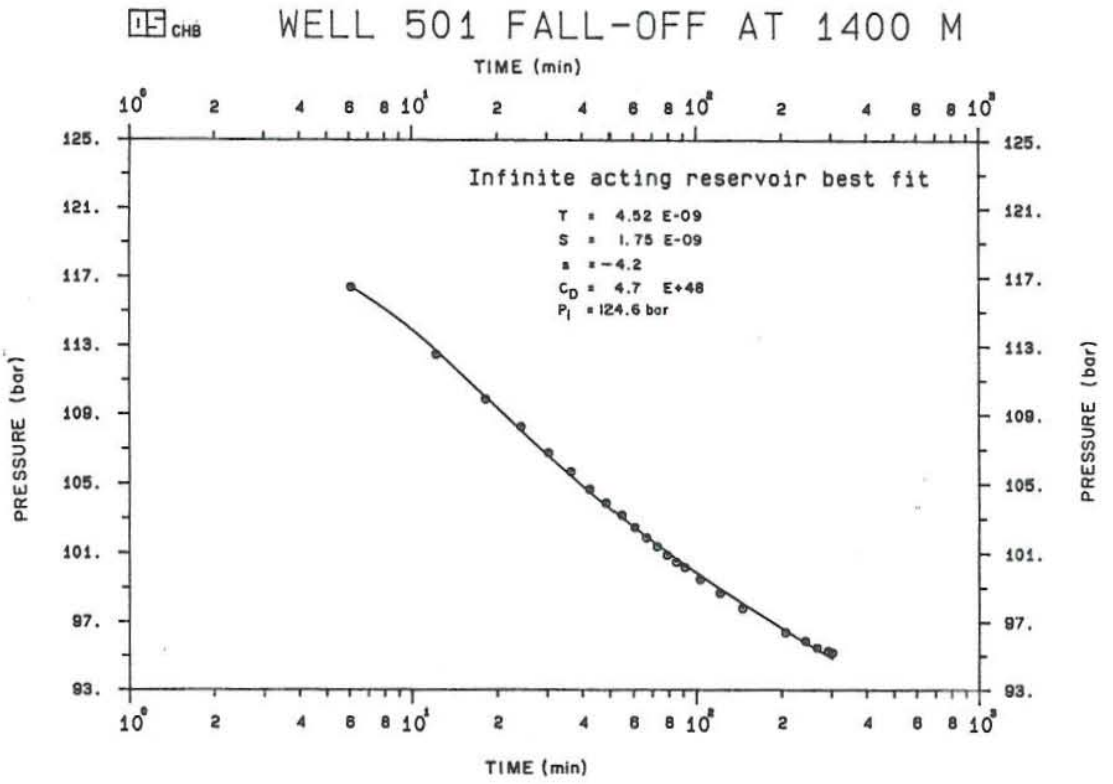

Fig. 15. Analytical infinite acting reservoir fit of pressure fall-off at 1400 m in well 501.

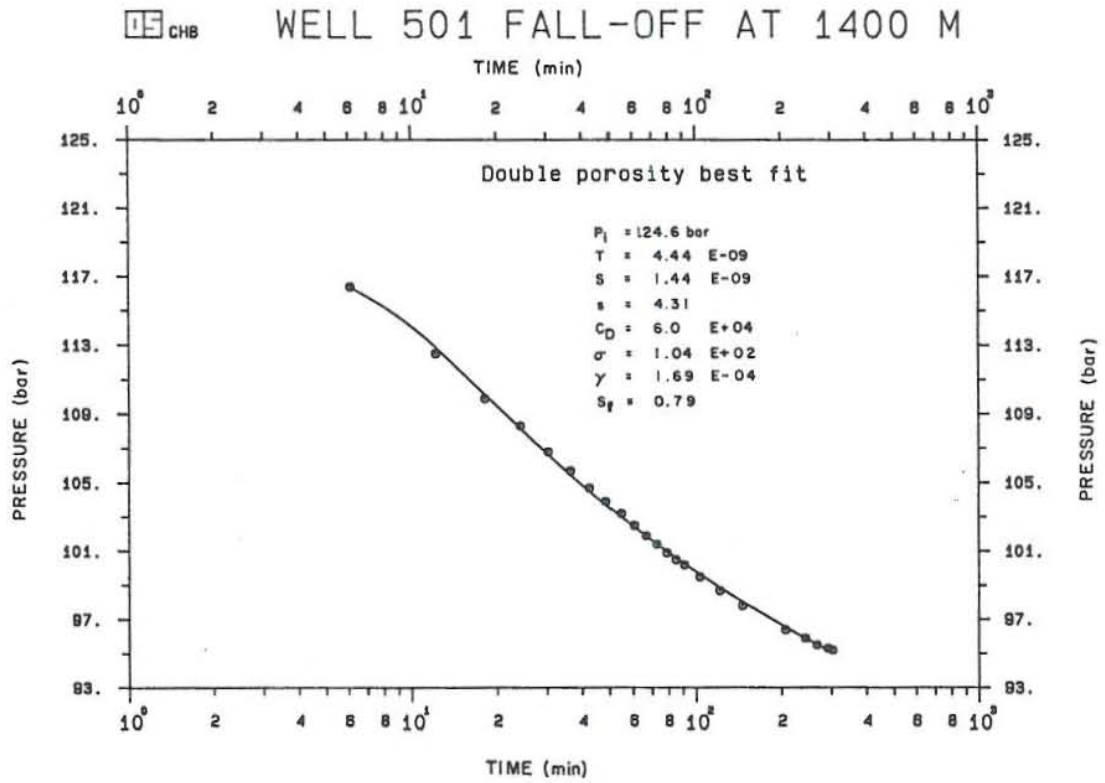

Fig. 16. Analytical double porosity fit of pressure fall-off at 1400 m in well 501.

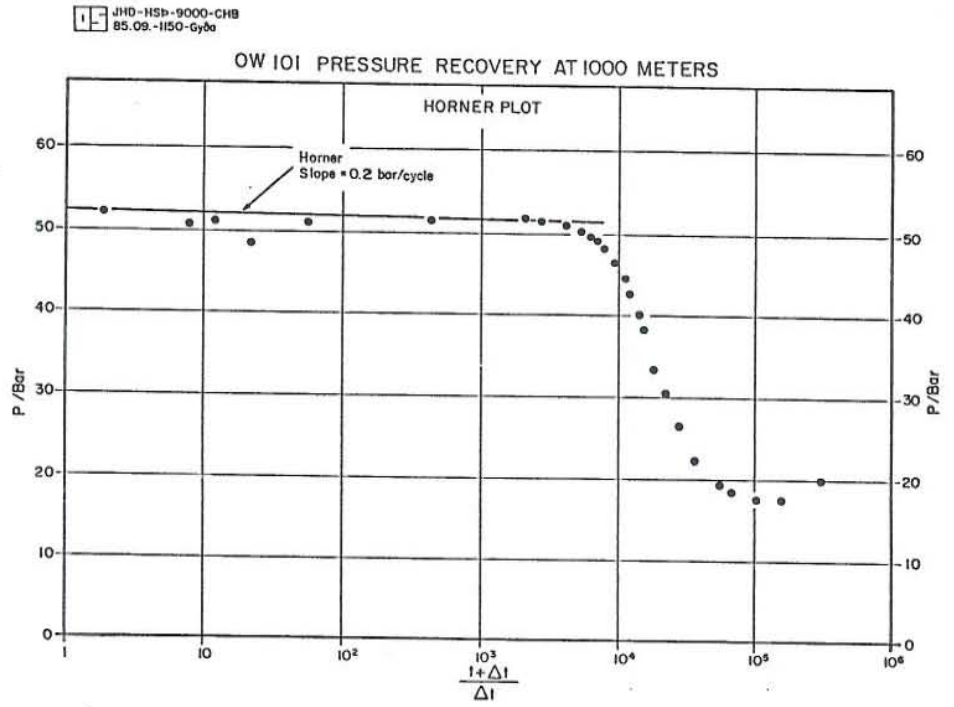

Fig. 17. Horner plot of pressure recovery at 1000 m in well 101.

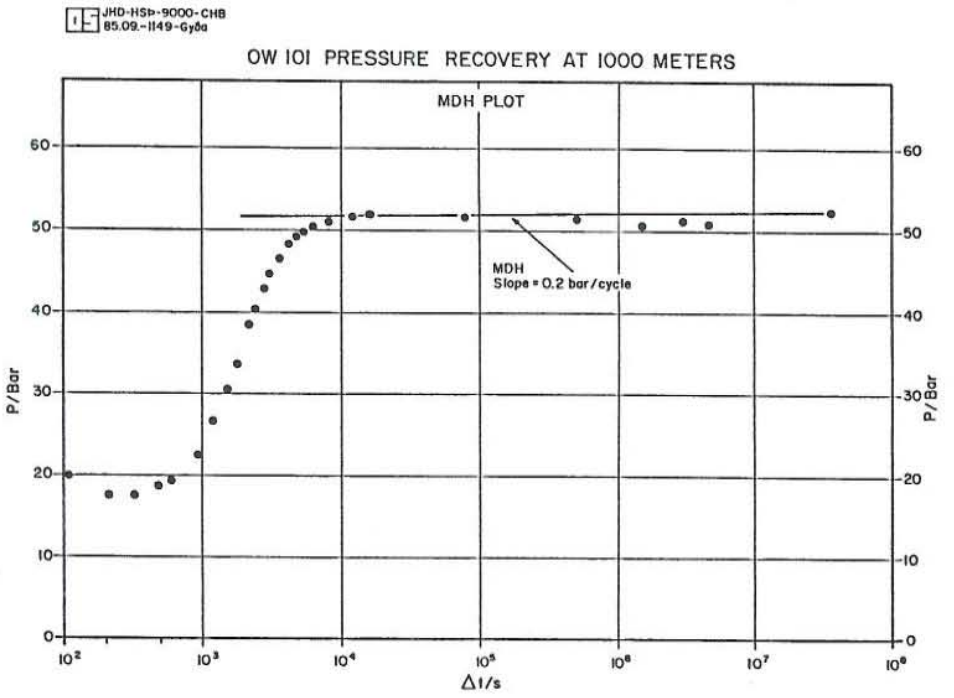

Fig. 18. MDH plot of pressure recovery at 1000 m in well 101.

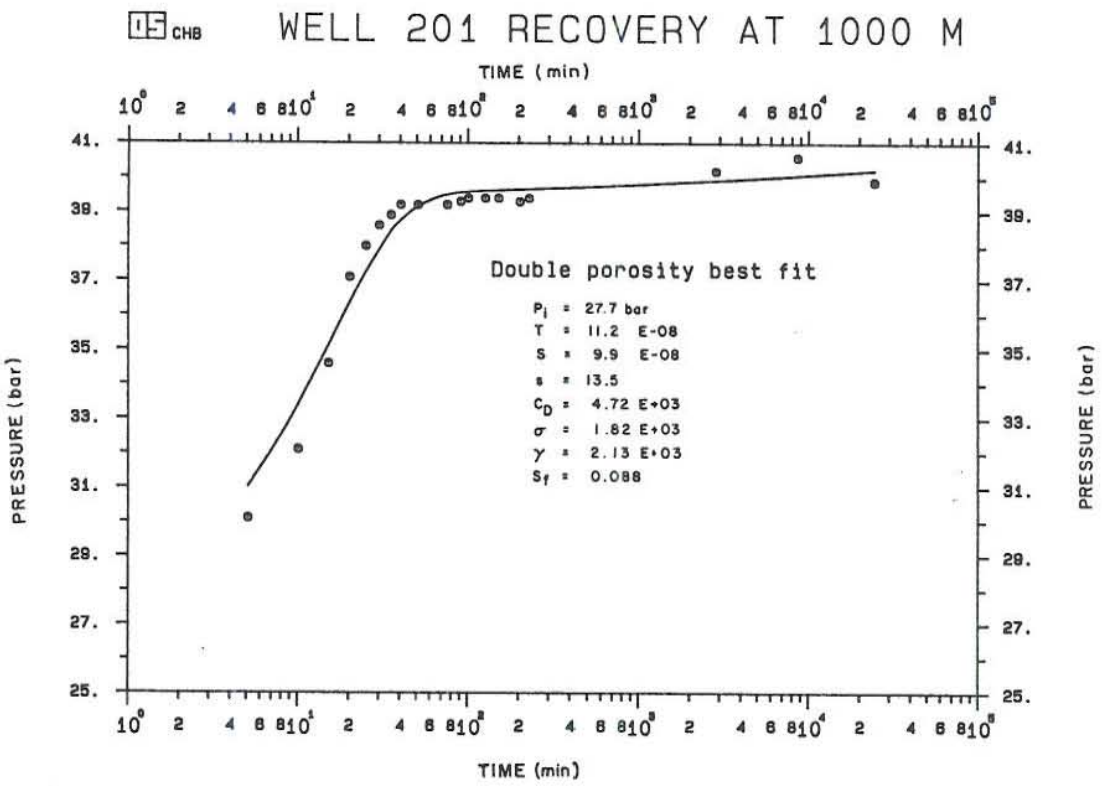

Fig. 19. Analytical double porosity fit of pressure recovery at 1000 m in well 201.

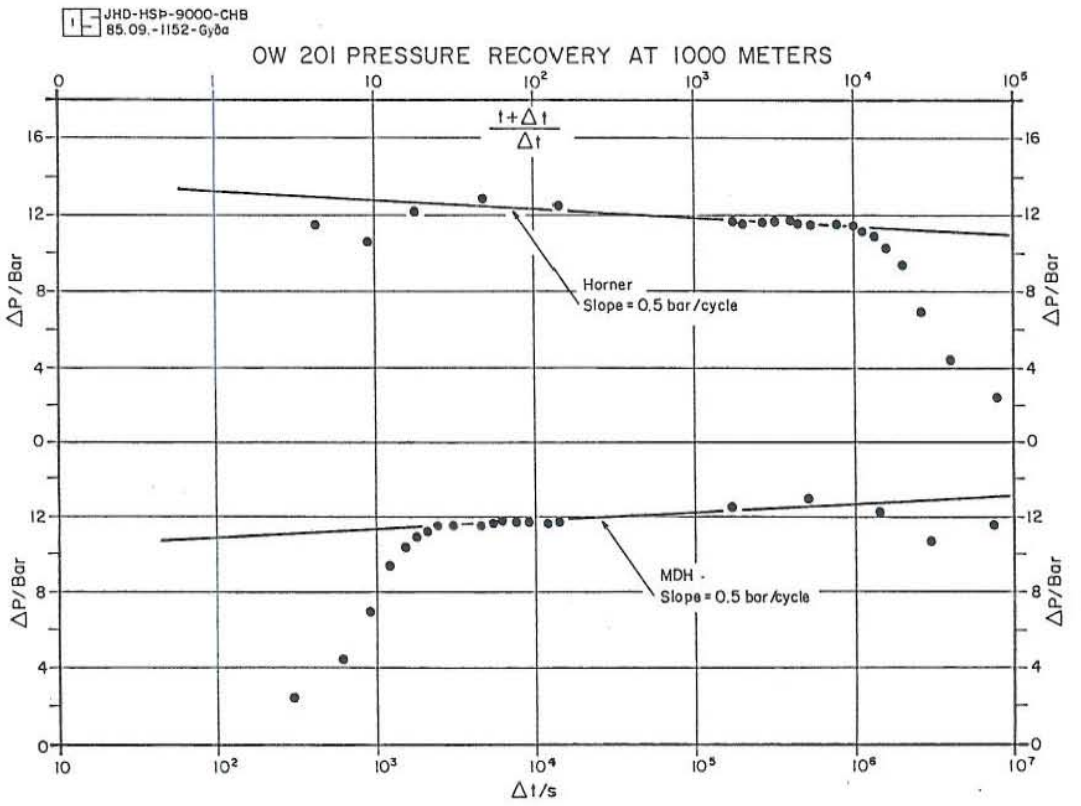

Fig. 20. Semilog plot of pressure recovery at 1000 m in well 201.

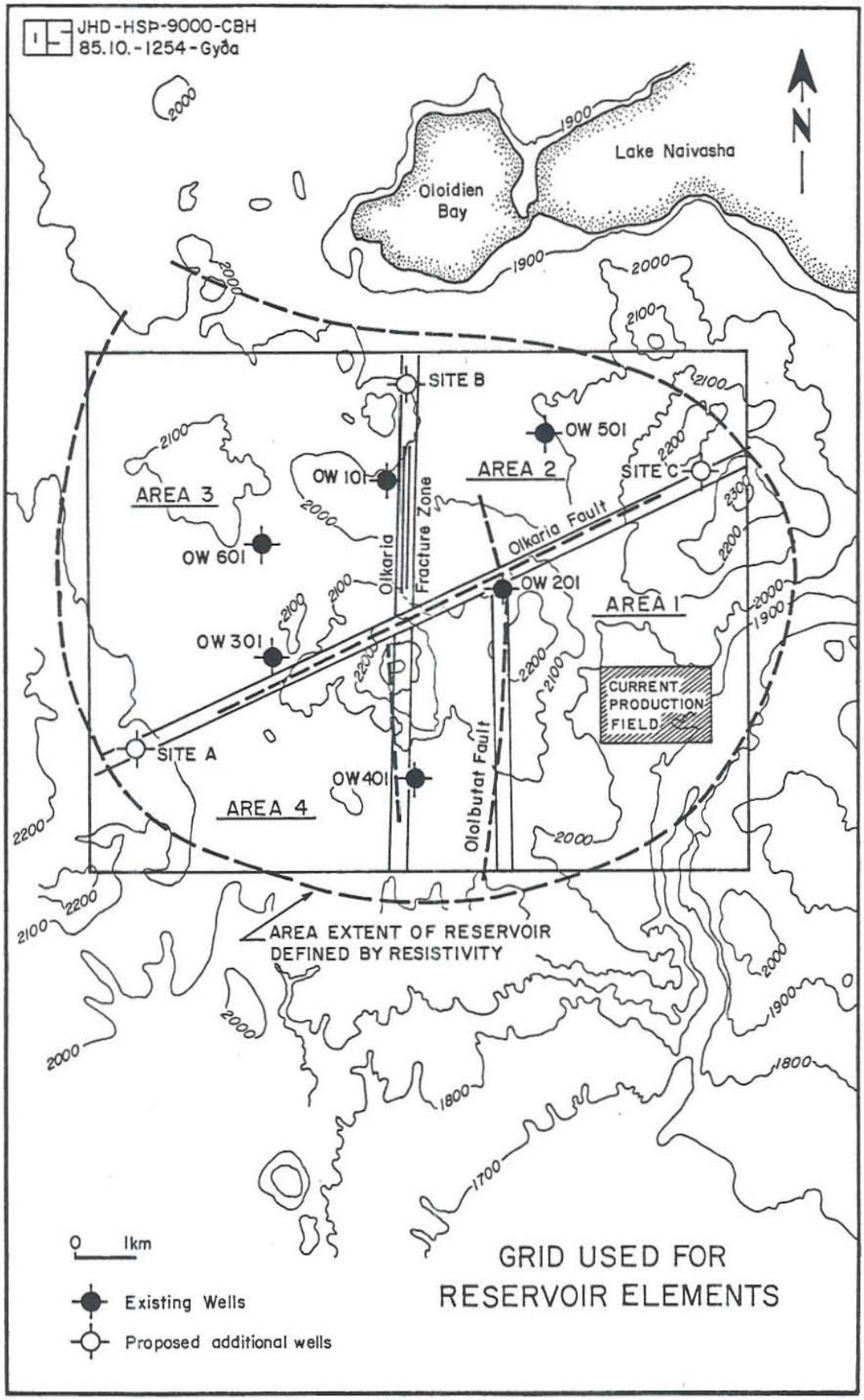

Fig. 21. Aerial division of the reservoir area.

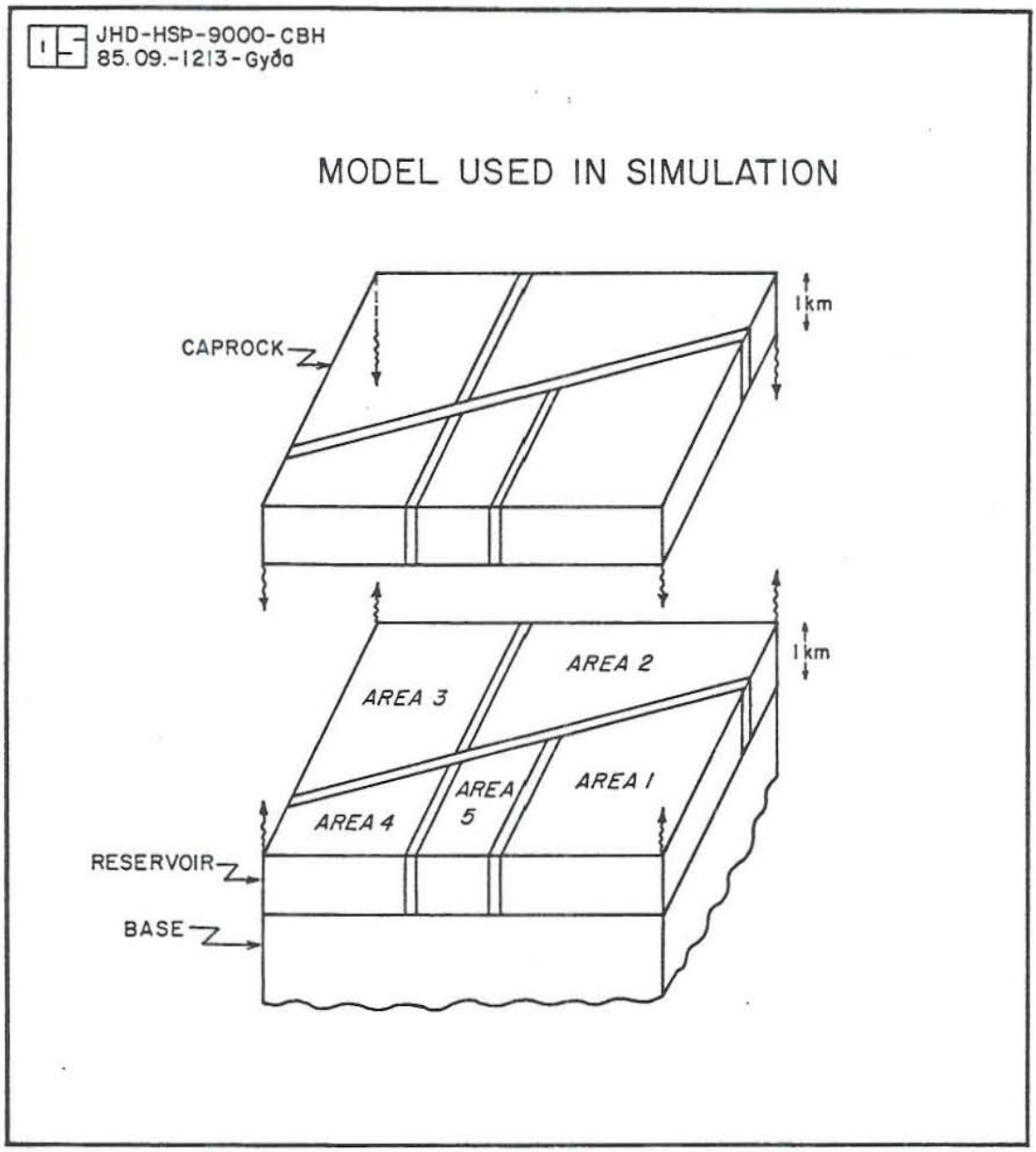

Fig. 22. Three dimensional model used.

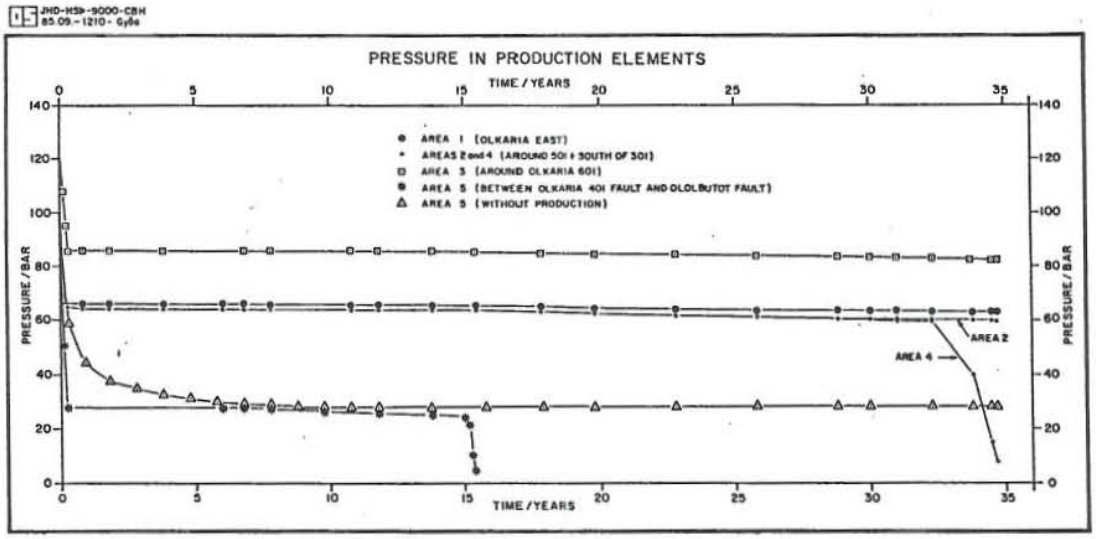

Fig. 23. Pressure in production elements.

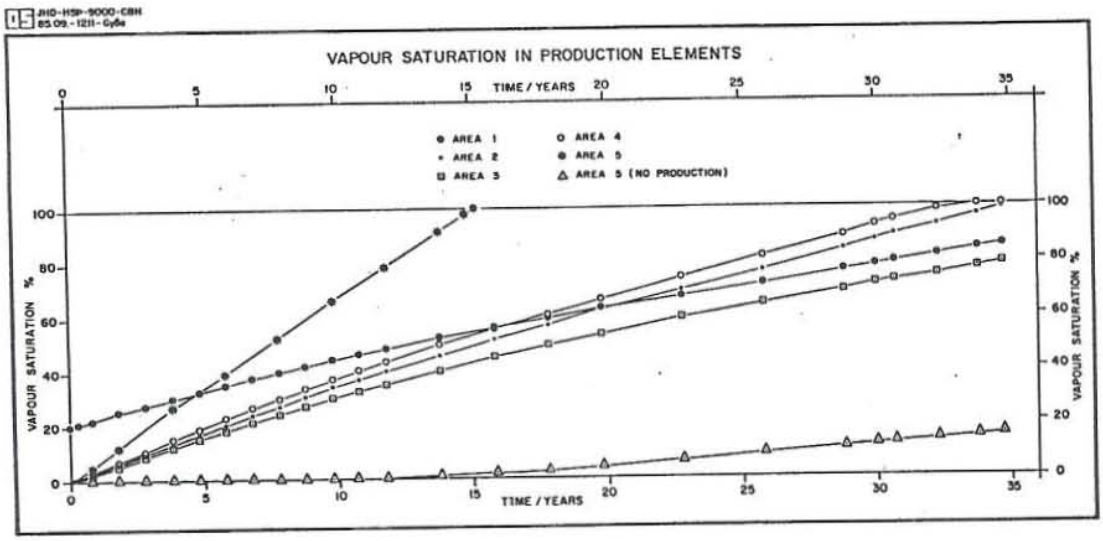

Fig. 24. Vapour saturation in production elements.

JHD-HSP-9000-CBH
85.09.-1212 - Gyða

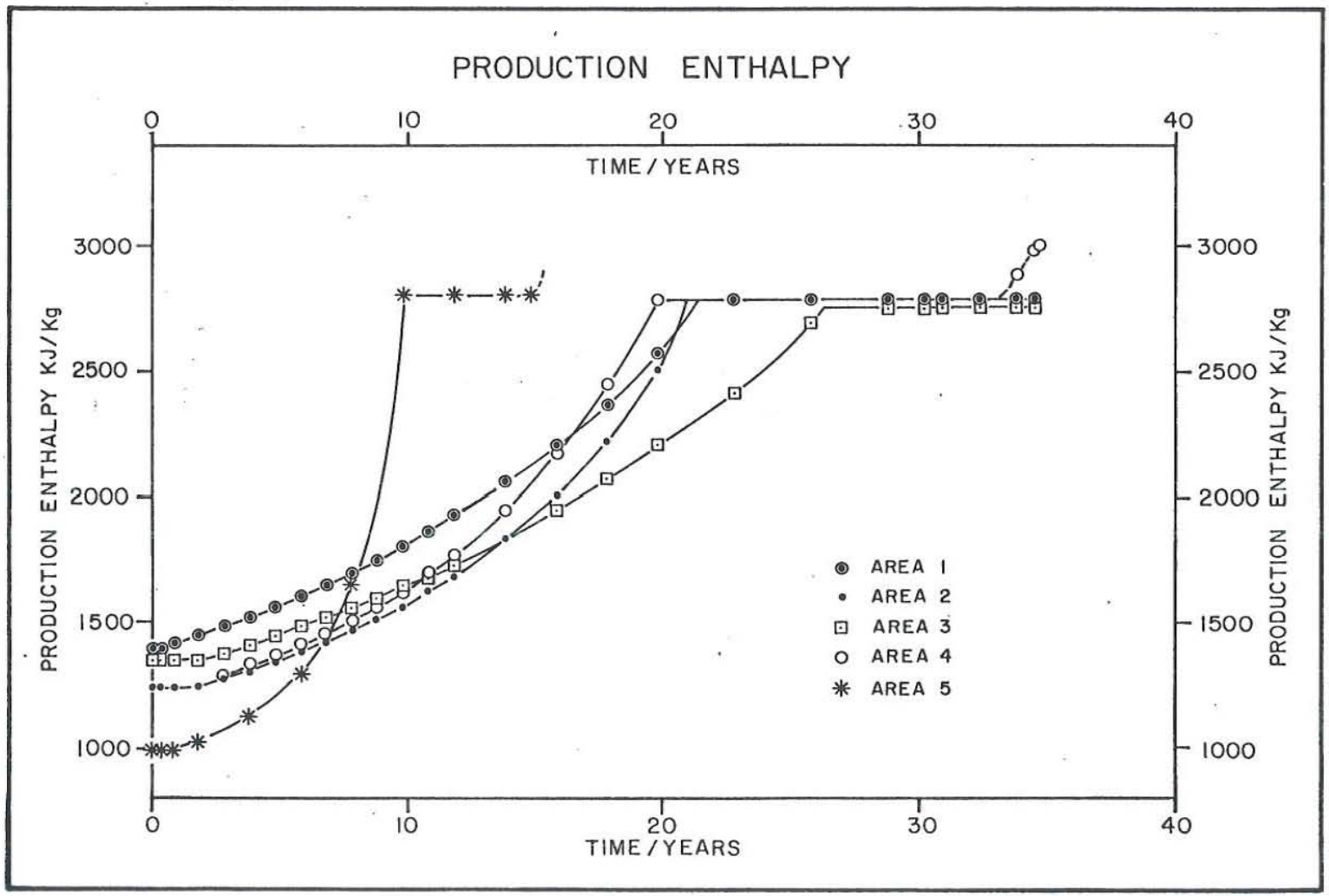

Fig. 25. Production enthalpy.

TABLE 1: Summary of data from Olkaria East wells

Well no.	Transmissivity m^3/Pas/E-8			History match	Anlyses by KRTA (12)	Average output
	Injectivity index	Fall-off	Recovery	kh/dm	kh/dm	kg/s
2	-	-	-	2.75	-	13.9
3	-	-	-	0.75	-	5.6
4	-	-	-	1.50	-	-
5	-	-	-	3.00	-	12.5
6	-	-	0.85	3.50	0.85(r)	6.9
7	-	-	-	1.25	-	4.2
8a	4.0	2.8	2.3	0.45	3.5(f)	5.0
9	-	-	-	1.00	1.5(r)	3.6
10	-	1.9	-	2.15	-	11.1
11	8.7	-	1.6	4.00	-	8.3
12	14.4	-	2.3	4.50	2.3(r)	14.7
13	4.6	-	5.7	2.8	1.1(r)	6.4
14	3.6	-	2.0	2.2	1.3(r)	6.4
15	3.9	-	1.8	8.8	1.4(r)	10.0
16	4.5	-	4.1	8.5	4.1(r)	18.9
17	3.3	0.80	0.30	4.0	0.30(r)	5.6
18	5.8	1.70	1.3	3.0	0.68(r)	10.0
19	2.1	0.40	0.06	1.5	0.16r/2.0f	9.7
20	5.4	1.10	0.4-1.4	1.75	-	7.2
21	5.2	0.65	1.5-4.9	1.75	0.29r/6.1f	5.6
22	7.2	1.00	4.0-13.0	2.0	-	6.9
23	3.4-5.5	2.10	3.9-5.5	1.5	2.7f	6.7
24	3.9	4.00	1.5-2.9	-	0.97r/5.3f	9.7
25	2.8	2.1	3.3	-	8.4f	11.1
26	7.5	2.1	-	-	3.5f	13.9

TABLE 2: Results of transient pressure analyses, well 101

Type of test	Type of analyses	T/E-08 m3/Pas	S/E-08 m/Pa	CD	s
Injectivity	Injectivity Index	5.5	-	-	-
Fall-off at 1200 m	Analytical infinite acting	4.8	0.60	1.2E+4	-3.0
	Analytical double porosity	4.8	0.69	1.1E+4	-3.0
	Type curve	8.0	1.00	1.0E+4	0
	MDH	4.2			
	Horner	3.7			
	KPC (Horner)	3.6			
Drawdown at 1000 m	Productivity Index	0.5			
	MDH	17.9			
Recovery at 1000 m	Horner	17.9			
	KPC (Horner)	0.02			

TABLE 3: Results of transient pressure analyses, well 201

Type of test	Type of analyses	T/E-8 m3/Pas	S/E-8 m/Pa	CD	s
Injectivity	Injectivity Index	1.83	-	-	-
Fall-off at 1900 m	Analytical infinite acting	2.2	2.7	1.3E+3	10
	Analytical double porosity	2.6	2.3	2.3E+3	13
	Type curve	4.0	0.06	1.0E+5	20
	MDH	2.1			
	Horner	2.2			
	KPC (Horner)	0.17			
Drawdown at 1000 m	Poductivity Index	5.0	-	-	-
Recovery at 1000 m	Analytical double porosity	11.2	9.9	4.7E+3	13.5
	MDH	16.4			
	Horner	16.4			
	KPC (Horner)	12.9			

TABLE 4: Results of transient pressure analyses, well 301

Injectivity	Injectivity index >4.8	
Fall-off at 1000 m	MDH/Horner	No straight line

TABLE 5: Results of transient pressure analyses, well 401

Type of test	Type of analyses	T/E-8 m3/Pas	S/E-8 m/Pa	CD	s
Injectivity	Injectivity Index	>.97			
Fall-off at 1000 m	Analytical infinite acting	2.6	0.71	1.5E+4	6.6
	Analytical double porosity	1.9	0.25	4.3E+4	3.6
	Type curve	2.3	1.0	1.0E+4	5.0
	MDH 2.0				
	Horner	1.5			
	KPC (Horner)	0.33			
Fall-off at 1100 m	Analytical infinite acting	2.4	1.7	1.5E+4	5.5
	Analytical double porosity	1.8	3.5	4.3E+4	2.8
	Type curve	4.3	0.59	1.0E+5	5.0
	MDH	0.41			
	Horner	0.35			
	KPC (Horner)	0.31			

TABLE 6: Results of transient pressure analyses, well 501

Type of test	Type of analyses	T/E-8 m3/Pas	S/E-8 m/Pa	CD	s
Injectivity	Injectivity Index	0.84-4.0			
Fall-off at 1300 m	Analytical infinite acting	0.99	0.18	7.0E+4	-3.5
	Analytical double porosity	0.69	0.16	6.0E+4	-4.6
	Type curve	0.75	0.08	1.0E+5	-5.0
	MDH	1.18			
	Horner	0.79			
	KPC (Horner)	0.78			
Fall-off at 1400 m	Analytical infinite acting	0.45	0.17	4.7E+4	-4.2
	Analytical double porosity	0.44	0.14	6.0E+4	-4.3
	Type curve	0.39	0.07	1.0E+5	-5.0
	MDH	0.70			
	Horner	0.54			
	KPC (Horner)	0.45			

TABLE 7: Results of semilog analyses of fall-off tests

Well no.	Depth monitored /meters	Type of analyses	Slope of plot bar/cycle	T/E-8 m3/Pas	Duration of fall-off step/s	Start of semilog line/s
101	1000	MDH	1.2	4.2	2.44E+3	>5.0E+2
	-	Horner	1.35	3.7	-	-
201	1900	MDH	2.2	2.1	3.60E+3	>1.7E+3
	-	Horner	2.1	2.2	-	-
401	1000	MDH	2.6	2.0	7.8E+3	>2.2E+3
	-	Horner	3.4	1.5	-	-
401	1100	MDH	12.0	0.41	7.1E+3	>4.0E+3
	-	Horner	14.0	0.35	-	-
501	1300	MDH	4.3	1.18	2.87E+4	>7.0E+3
	-	Horner	6.4	0.79	-	-
501	1400	MDH	5.9	0.70	1.82E+4	>1.2E+4
	-	Horner	7.6	0.54	-	-

TABLE 8: Fall-off data from well 501 at 1300 m

Date: 84-12-19 Measured data:

Time min	Pressure bar	Q l/s
0.0	106.40	27.67
7.4	98.30	0.00
14.8	95.30	0.00
22.2	93.60	0.00
29.6	92.30	0.00
36.9	91.30	0.00
44.3	90.50	0.00
59.1	89.40	0.00
73.9	88.60	0.00
88.7	88.00	0.00
103.5	87.50	0.00
133.0	86.80	0.00
177.0	86.10	0.00
237.0	85.50	0.00
266.0	85.20	0.00
296.0	85.00	0.00
355.0	84.70	0.00
384.0	84.60	0.00
443.0	84.40	0.00
479.0	84.30	0.00

TABLE 9: Computer fit to infinite acting system for well 501 fall-off at 1300 m

Date: 84-12-19 Radius of hole (m) 0.108.
Results of infinite acting reservoir interpretation.

Initial pressure (bar):	1.064E+02F
Transmissivity T (m^3/Pas):	9.918E-09
Formation storage S (m/Pa):	1.820E-09
Wellbore skin s:	-3.527E+00
Wellbore storage CD:	6.988E+04

No.	Measured pressure bar	Calculated pressure bar	Deviation from measured bar	%
1	0.9830E+02	0.9878E+02	-0.4803E+00	0.5
2	0.9530E+02	0.9527E+02	0.2980E-01	0.0
3	0.9360E+02	0.9327E+02	0.3319E+00	0.4
4	0.9230E+02	0.9198E+02	0.3220E+00	0.3
5	0.9130E+02	0.9108E+02	0.2191E+00	0.2
6	0.9050E+02	0.9040E+02	0.1032E+00	0.1
7	0.8940E+02	0.8942E+02	-0.1514E-01	0.0
8	0.8860E+02	0.8872E+02	-0.1211E+00	0.1
9	0.8800E+02	0.8819E+02	-0.1879E+00	0.2
10	0.8750E+02	0.8776E+02	-0.2559E+00	0.3
11	0.8680E+02	0.8708E+02	-0.2827E+00	0.3
12	0.8610E+02	0.8635E+02	-0.2484E+00	0.3
13	0.8550E+02	0.8562E+02	-0.1246E+00	0.1
14	0.8520E+02	0.8534E+02	-0.1440E+00	0.2
15	0.8500E+02	0.8509E+02	-0.8651E-01	0.1
16	0.8470E+02	0.8465E+02	0.4692E-01	0.1
17	0.8460E+02	0.8447E+02	0.1326E+00	0.2
18	0.8440E+02	0.8413E+02	0.2686E+00	0.3
19	0.8430E+02	0.8395E+02	0.3512E+00	0.4

Variance:	5.4E-02
Mean deviation:	0.22 %

TABLE 10: Computer fit to double porosity model for well 501 fall-off at 1300 m

Date : 84-12-19 Radius of hole (m) 0.108.
Results of double porosity interpretation.

Inital pressure (bar):	1.064E+02F
Transmissivity T (m^3/Pas):	6.929E-09
Formation storage S (m/Pa):	1.613E-09
Wellbore skin s:	-4.568E+00
Wellbore storage CD:	5.983E+04
Relative fracture storativity sigma:	1.034E+02
Interporosity flow coefficient gamma:	2.717E-04
Fracture skin sf:	6.250E-01

No.	Measured pressure bar	Calculated pressure bar	Deviation from measured bar	%
1	0.9830E+02	0.9830E+02	0.4302E-02	0.0
2	0.9530E+02	0.9546E+02	-0.1551E+00	0.2
3	0.9360E+02	0.9350E+02	0.1002E+00	0.1
4	0.9230E+02	0.9219E+02	0.1122E+00	0.1
5	0.9130E+02	0.9124E+02	0.5847E-01	0.1
6	0.9050E+02	0.9050E+02	0.5750E-03	0.0
7	0.8940E+02	0.8941E+02	-0.8477E-02	0.0
8	0.8860E+02	0.8863E+02	-0.2822E-01	0.0
9	0.8800E+02	0.8803E+02	-0.3215E-01	0.0
10	0.8750E+02	0.8756E+02	-0.5669E-01	0.1
11	0.8680E+02	0.8684E+02	-0.3923E-01	0.0
12	0.8610E+02	0.8611E+02	-0.5715E-02	0.0
13	0.8550E+02	0.8545E+02	0.4849E-01	0.1
14	0.8520E+02	0.8522E+02	-0.1993E-01	0.0
15	0.8500E+02	0.8502E+02	-0.1945E-01	0.0
16	0.8470E+02	0.8471E+02	-0.9065E-02	0.0
17	0.8460E+02	0.8459E+02	0.1318E-01	0.0
18	0.8440E+02	0.8438E+02	0.1767E-01	0.0
19	0.8430E+02	0.8428E+02	0.1987E-01	0.0

Variance:	3.2E-03
Mean deviation:	0.04 %